

Content

Fig. S1: $^1\text{H-NMR}$ of the black residue after heating **3** at 120 °C for 3 h under inert conditions at atmospheric pressure.

Fig. S2: ATR-IR spectrum of $\text{Fe}(\text{acac})_2(\text{TMEDA})$.

Fig. S3: ATR-IR spectrum of $\text{Fe}(\text{tfac})_2(\text{TMEDA})$ **1**.

Fig. S4: ATR-IR spectrum of $\text{Fe}(\text{hfac})_2(\text{TMEDA})$.

Fig. S5: ATR-IR spectrum of $\text{Ni}(\text{acac})_2(\text{TMEDA})$.

Fig. S6: ATR-IR spectrum of $\text{Ni}(\text{tfac})_2(\text{TMEDA})$ **2**.

Fig. S7: ATR-IR spectrum of $\text{Ni}(\text{hfac})_2(\text{TMEDA})$.

Fig. S8: ATR-IR spectrum of $\text{Cu}(\text{tfac})_2(\text{TMEDA})$ **3**.

Fig. S9: ATR-IR spectrum of $\text{Cu}(\text{hfac})_2(\text{TMEDA})$.

Fig. S10: ATR-IR spectrum of $\text{Zn}(\text{acac})_2(\text{TMEDA})$.

Fig. S11: ATR-IR spectrum of $\text{Zn}(\text{tfac})_2(\text{TMEDA})$ **4**.

Fig. S12: ATR-IR spectrum of $\text{Zn}(\text{hfac})_2(\text{TMEDA})$.

Fig. S13: Isothermal TGA curves (125 °C) for $\text{M}(\text{acac})_2$, $\text{M}(\text{acac})_2(\text{TMEDA})$, $\text{M}(\text{tfac})_2(\text{TMEDA})$ and $\text{M}(\text{hfac})_2(\text{TMEDA})$ ($\text{M} = \text{Fe}$ (a), Ni (b), Cu (c) and Zn (d)).

Fig. S14: XRD of **1**.

Fig. S15: XRD of **2**.

Fig. S16: XRD of **3**.

Fig. S17: XRD of **4**.

Fig. S18: 3D model of the MOCVD reactor.

Fig. S19: SEM of **1_Si** at 300 °C (a), 400 °C (b) and 500 °C (c).

Fig. S20: SEM of **1_Si** at 300 °C (a), 400 °C (b) and 500 °C (c).

Fig. S21: SEM of **1_Si** at 300 °C (a), 400 °C (b) and 500 °C (c).

Fig. S22: SEM of **1_Si** at 300 °C (a), 400 °C (b) and 500 °C (c).

Fig. S23: EDX spectrum of **1_AI**

Fig. S24: EDX spectrum of **2_AI**

Fig. S25: EDX spectrum of **3_AI**

Fig. S26: EDX spectrum of **4_AI**

Fig. S27: XRD of **1_Si**.

Fig. S28: XRD of **2_Si**.

Fig. S29: XRD of **3_Si**.

Fig. S30: XRD of **4_Si**.

Fig. S31: SEM image of **1_AI**.

Fig. S32: Cross section SEM image of **1_AI**.

Fig. S33: SEM image of **2_AI**.

Fig. S34: Cross section SEM image of **2_AI**.

Fig. S35: SEM image of **3_AI**.

Fig. S36: Cross section SEM image of **3_AI**.

Fig. S37: SEM image of **4_AI**.

Fig. S38: Cross section SEM image of **4_AI**.

Fig. S39: XPS of **1_AI**. Survey (a), Fe 2p (b), O 1s (c) and C 1s (d).

Fig. S40: XPS of **1_AI** after calcination. Survey (a), Fe 2p (b), O 1s (c) and C 1s (d).

Fig. S41: XPS of **2_AI**. Survey (a), Ni 2p (b), O 1s (c) and C 1s (d).

Fig. S42: XPS of **2_AI** after calcination. Survey (a), Ni 2p (b), O 1s (c) and C 1s (d).

Fig. S43: XPS of **3_AI**. Survey (a), Cu 2p (b), O 1s (c) and C 1s (d).

Fig. S44: XPS of **3_AI** after calcination. Survey (a), Cu 2p (b), O 1s (c) and C 1s (d).

Fig. S45: Cu LMM spectra of **3_AI** before and after calcination.

Fig. S46: XPS of **4_AI**. Survey (a), Zn 2p (b), O 1s (c) and C 1s (d).

Fig. S47: XPS of **4_AI** after calcination. Survey (a), Zn 2p (b), O 1s (c) and C 1s (d).

Fig. S48: Zn LMM spectra of **4_AI** before and after calcination.

Tab. S1: Crystal Data and Structure Refinement for **1**.

Tab. S2: Crystal Data and Structure Refinement for **2**.

Tab. S3: Crystal Data and Structure Refinement for **3**.

Tab. S4: Crystal Data and Structure Refinement for **4**.

Tab. S5: Overview on intermolecular contacts in **1-4**.

Tab. S6: Experimental conditions.

Tab. S7: Calculation of the mod. Auger parameter for **3_AI**

Tab. S8: Calculation of the mod. Auger parameter for **4_AI**

Tab. S1: Crystal Data and Structure Refinement for **1**.

Empirical Formula	C ₁₆ H ₂₄ F ₆ N ₂ O ₄ Fe
Formular weight	478.22 Da
Density (calculated)	1.509 g · cm ⁻³
F (000)	984
Temperature	100(2) K
Crystal size	0.322 x 0.156 x 0.098 mm
Crystal appearance	red tablet
Wavelength (MoK _α)	0.71073 Å
Crystal system	Monoclinic
Space group	<i>P</i> 2 ₁ / <i>c</i>
Unit cell volume	a = 8.2798(9) Å b = 26.236(3) Å c = 10.1171(11) Å α = 90° β = 106.7333(16)° γ = 90°
Unit cell volume	2104.6(4) Å ³
Z	4
Cell measurement reflections used	9940
θ range for cell measurement	2.24° to 24.80°
Diffractometer used for measurement	Bruker D8 KAPPA II (APEX II detector)
Diffractometer control software	BRUKER APEX3 (v2019.1-0)
Measurement method	Data collection strategy APEX 3/QUEEN
θ range for data collection	2.613° to 30.749°
Completeness to θ = 25.242° (to θ _{max})	99.9% (99.5%)
Index ranges	-11 ≤ h ≤ 11 0 ≤ k ≤ 37 0 ≤ l ≤ 14
Computing data reduction	BRUKER APEX3 (v2019.1-0)
Absorption correction	Semi-empirical form equivalents
Absorption coefficient	0.792 mm ⁻¹
Absorption correction computing	TWINABS
Max./min. transmission	0.75/0.61

R_{merge} before/after correction	0.0678/0.0551 and 0.0902/0.0653
Computing structure solution	BRUKER APEX3 (v2019.1-0)
Computing structure refinement	SHELXL-2017/1 (Sheldrick, 2017)
Refinement method	Full-matrix least-squares on F^2
Reflections collected	117073
Independent reflections	6534 ($R_{\text{int}} = 0.0797$)
Reflections with $I > 2\sigma(I)$	5293
Data / restraints / parameter	6534 / 142 / 324
Goodness-of-fit on F^2	1.075
Weighting details	$\omega = 1/[\sigma^2(F_o^2) + (0.0395P)^2 + 0.9427P]$ where $P = (F_o^2 + 2F_c^2)/3$
R indices [$I > 2\sigma(I)$]	$R1 = 0.0416$ $\omega R2 = 0.0866$
R indices [all data]	$R1 = 0.0605$ $\omega R2 = 0.0931$
Largest diff. peak and hole	0.591 and -0.299 \AA^{-3}

Tab. S2: Crystal Data and Structure Refinement for **2**.

Empirical Formula	C ₁₆ H ₂₄ F ₆ N ₂ O ₄ Ni
Formular weight	481.08 Da
Density (calculated)	1.552 g · cm ⁻³
F (000)	992
Temperature	100(2) K
Crystal size	0.350 x 0.216 x 0.208 mm
Crystal appearance	blue tablet
Wavelength (MoK _α)	0.71073 Å
Crystal system	Monoclinic
Space group	<i>P</i> 2 ₁ / <i>c</i>
Unit cell volume	a = 8.1121(5) Å b = 20.0344(13) Å c = 12.6691(8) Å α = 90° β = 91.0753(15)° γ = 90°
Unit cell volume	2058.6(2) Å ³
Z	4
Cell measurement reflections used	9716
θ range for cell measurement	3.17° to 33.32°
Diffractometer used for measurement	Bruker D8 KAPPA II (APEX II detector)
Diffractometer control software	BRUKER APEX3 (v2019.1-0)
Measurement method	Data collection strategy APEX 3/QUEEN
θ range for data collection	1.902° to 33.425°
Completeness to θ = 25.242° (to θ _{max})	99.9% (99.8%)
Index ranges	-12 ≤ h ≤ 12 -30 ≤ k ≤ 31 -19 ≤ l ≤ 13
Computing data reduction	BRUKER APEX3 (v2019.1-0)
Absorption correction	Semi-empirical form equivalents
Absorption coefficient	1.020 mm ⁻¹
Absorption correction computing	SADABS
Max./min. transmission	0.75/0.66

R_{merge} before/after correction	0.0445/0.0352
Computing structure solution	BRUKER APEX3 (v2019.1-0)
Computing structure refinement	SHELXL-2017/1 (Sheldrick, 2017)
Refinement method	Full-matrix least-squares on F^2
Reflections collected	82511
Independent reflections	8019 ($R_{\text{int}} = 0.0226$)
Reflections with $I > 2\sigma(I)$	7248
Data / restraints / parameter	8019 / 53 / 327
Goodness-of-fit on F^2	1.046
Weighting details	$\omega = 1/[\sigma^2(F_o^2) + (0.0353P)^2 + 0.6264P]$ where $P = (F_o^2 + 2F_c^2)/3$
R indices [$I > 2\sigma(I)$]	$R1 = 0.0245$ $\omega R2 = 0.0642$
R indices [all data]	$R1 = 0.0286$ $\omega R2 = 0.0667$
Largest diff. peak and hole	0.557 and -0.353 \AA^{-3}

Tab. S3: Crystal Data and Structure Refinement for **3**.

Empirical Formula	C ₁₆ H ₂₄ F ₆ N ₂ OCu
Formular weight	495.91 Da
Density (calculated)	1.541 g · cm ⁻³
F (000)	996
Temperature	100(2) K
Crystal size	0.362 x 0.325 x 0.110 mm
Crystal appearance	green plate
Wavelength (MoK _α)	0.71073 Å
Crystal system	Monoclinic
Space group	<i>P2₁/n</i>
Unit cell volume	a = 9.7772(10) Å b = 15.3822(16) Å c = 14.6761(15) Å α = 90° β = 108.4413(16)° γ = 90°
Unit cell volume	2093.9(4) Å ³
Z	4
Cell measurement reflections used	9810
θ range for cell measurement	2.56° to 32.98°
Diffractometer used for measurement	Bruker D8 KAPPA II (APEX II detector)
Diffractometer control software	BRUKER APEX3 (v2019.1-0)
Measurement method	Data collection strategy APEX 3/QUEEN
θ range for data collection	2.220° to 33.481°
Completeness to θ = 25.242° (to θ _{max})	100% (99.3%)
Index ranges	-15 ≤ h ≤ 15 -23 ≤ k ≤ 23 -22 ≤ l ≤ 22
Computing data reduction	BRUKER APEX3 (v2019.1-0)
Absorption correction	Semi-empirical form equivalents
Absorption coefficient	1.119 mm ⁻¹
Absorption correction computing	SADABS
Max./min. transmission	0.75/0.60

R_{merge} before/after correction	0.0647/0.0448
Computing structure solution	BRUKER APEX3 (v2019.1-0)
Computing structure refinement	SHELXL-2017/1 (Sheldrick, 2017)
Refinement method	Full-matrix least-squares on F^2
Reflections collected	70229
Independent reflections	8143 ($R_{\text{int}} = 0.0384$)
Reflections with $I > 2\sigma(I)$	6554
Data / restraints / parameter	8143 / 349 / 353
Goodness-of-fit on F^2	1.053
Weighting details	$\omega = 1/[\sigma^2(F_o^2) + (0.0348P)^2 + 0.9588P]$ where $P = (F_o^2 + 2F_c^2)/3$
R indices [$I > 2\sigma(I)$]	$R1 = 0.0291$ $\omega R2 = 0.0696$
R indices [all data]	$R1 = 0.0448$ $\omega R2 = 0.0782$
Largest diff. peak and hole	0.623 and -0.657 \AA^{-3}

Tab. S4: Crystal Data and Structure Refinement for **4**.

Empirical Formula	C ₁₆ H ₂₄ F ₆ N ₂ O ₄ Zn
Formular weight	487.74 Da
Density (calculated)	1.437 g · cm ⁻³
F (000)	1000
Temperature	100(2) K
Crystal size	0.541 x 0.359 x 0.190 mm
Crystal appearance	colourless tablet
Wavelength (MoK _α)	0.71073 Å
Crystal system	Monoclinic
Space group	<i>P</i> 2 ₁ / <i>c</i>
Unit cell volume	a = 8.323(19) Å b = 20.79(5) Å c = 13.03(3) Å α = 90° β = 90.27(4)° γ = 90°
Unit cell volume	2254(9) Å ³
Z	4
Cell measurement reflections used	4056
θ range for cell measurement	3.69° to 30.34°
Diffractometer used for measurement	Bruker D8 KAPPA II (APEX II detector)
Diffractometer control software	BRUKER APEX3 (v2019.1-0)
Measurement method	Data collection strategy APEX 2/COSMO
θ range for data collection	3.826° to 31.386°
Completeness to θ = 25.242° (to θ _{max})	98.8% (93.9%)
Index ranges	-9 ≤ h ≤ 11 -29 ≤ k ≤ 29 -19 ≤ l ≤ 18
Computing data reduction	BRUKER APEX3 (v2019.1-0)
Absorption correction	Semi-empirical form equivalents
Absorption coefficient	1.160 mm ⁻¹
Absorption correction computing	SADABS
Max./min. transmission	0.75/0.62

R_{merge} before/after correction	0.1676/0.0869
Computing structure solution	BRUKER APEX3 (v2019.1-0)
Computing structure refinement	SHELXL-2017/1 (Sheldrick, 2017)
Refinement method	Full-matrix least-squares on F^2
Reflections collected	43803
Independent reflections	6974 ($R_{\text{int}} = 0.0450$)
Reflections with $I > 2\sigma(I)$	5203
Data / restraints / parameter	6974 / 132 / 324
Goodness-of-fit on F^2	1.090
Weighting details	$\omega = 1/[\sigma^2(F_o^2) + (0.0475P)^2 + 1.6161P]$ where $P = (F_o^2 + 2F_c^2)/3$
R indices [$I > 2\sigma(I)$]	$R1 = 0.0538$ $\omega R2 = 0.1364$
R indices [all data]	$R1 = 0.0739$ $\omega R2 = 0.1459$
Largest diff. peak and hole	0.585 and -0.309 \AA^{-3}

Tab. S5: Overview on intermolecular contacts in **1-4**.

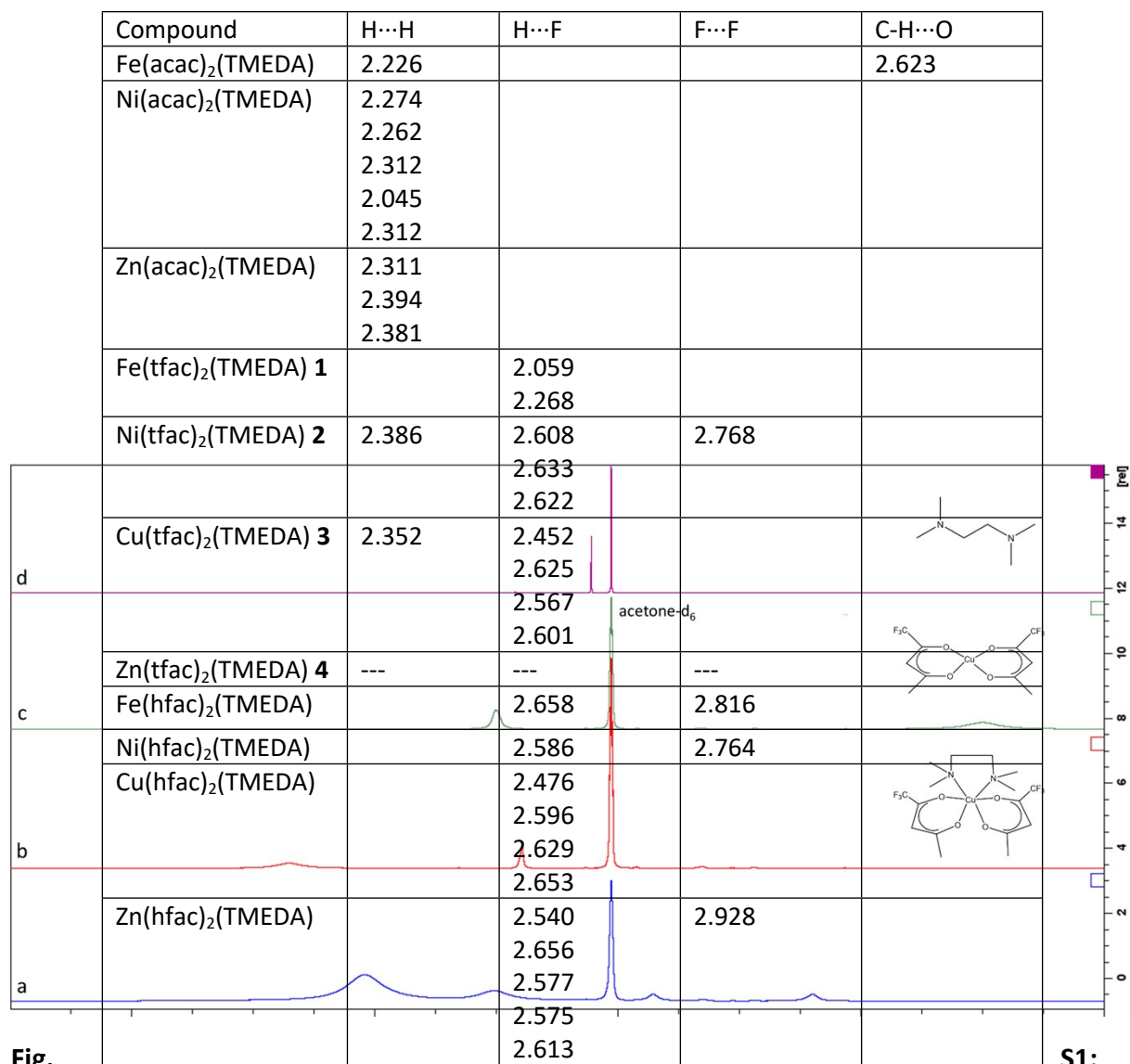


Fig.

S1:

¹H-NMR of the black residue after heating **3** at 120 °C for 3 h under inert conditions at atmospheric pressure. (a). The comparison with the spectrum of **3** (b) shows the complete degradation of the starting material. Further comparison with the spectra of Cu(tfac)₂ (c) and TMEDA (d) excludes the loss of TMEDA as decomposing pathway. All spectra were recorded in acetone-d₆.

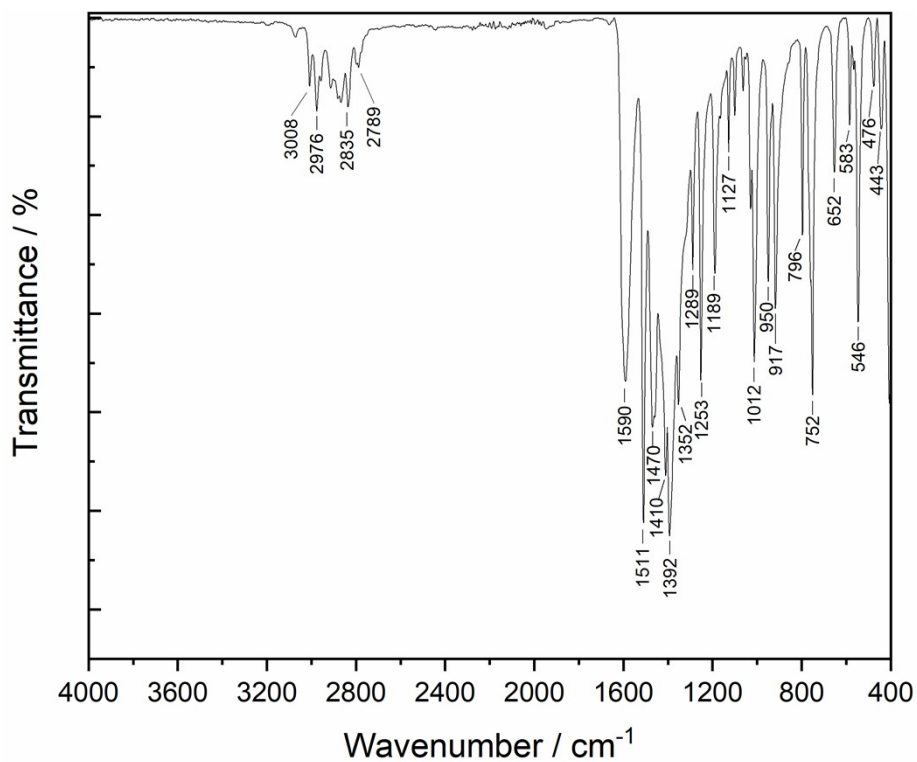


Fig. S2: ATR-IR spectrum of Fe(acac)₂(TMEDA).

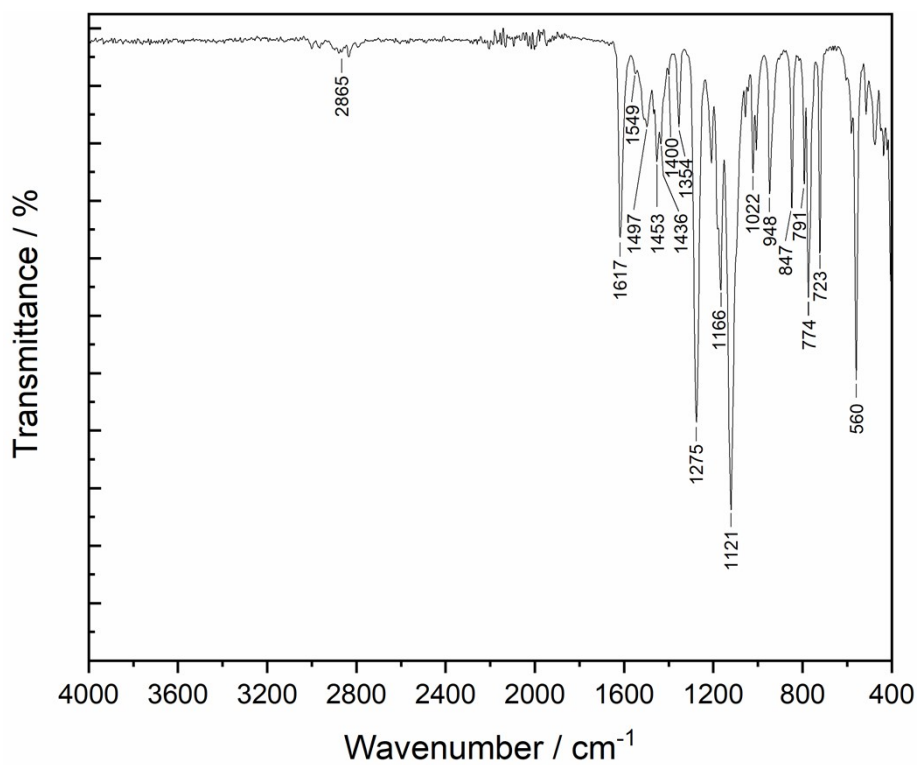


Fig. S3: ATR-IR spectrum of Fe(tfac)₂(TMEDA) 2.

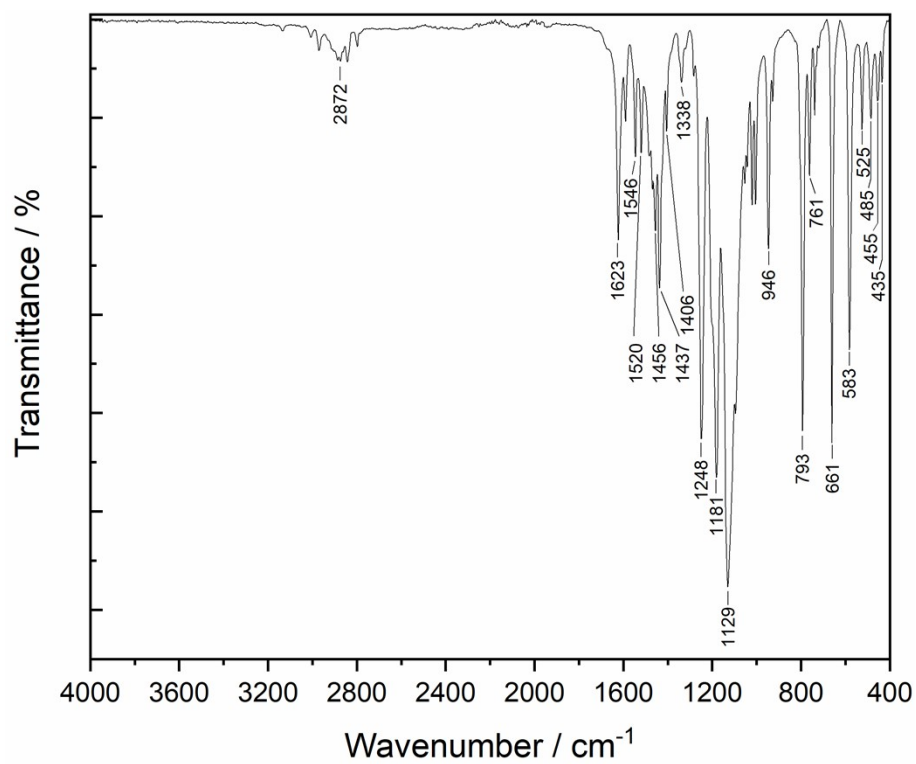


Fig. S4: ATR-IR spectrum of Fe(hfac)₂(TMEDA).

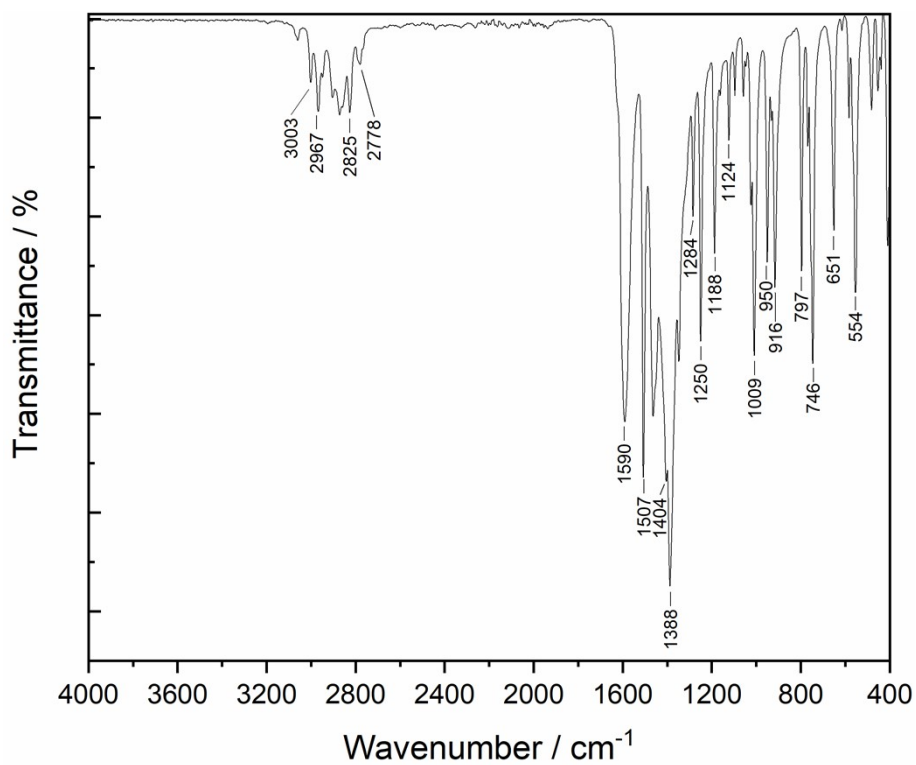


Fig. S5: ATR-IR spectrum of Ni(acac)₂(TMEDA).

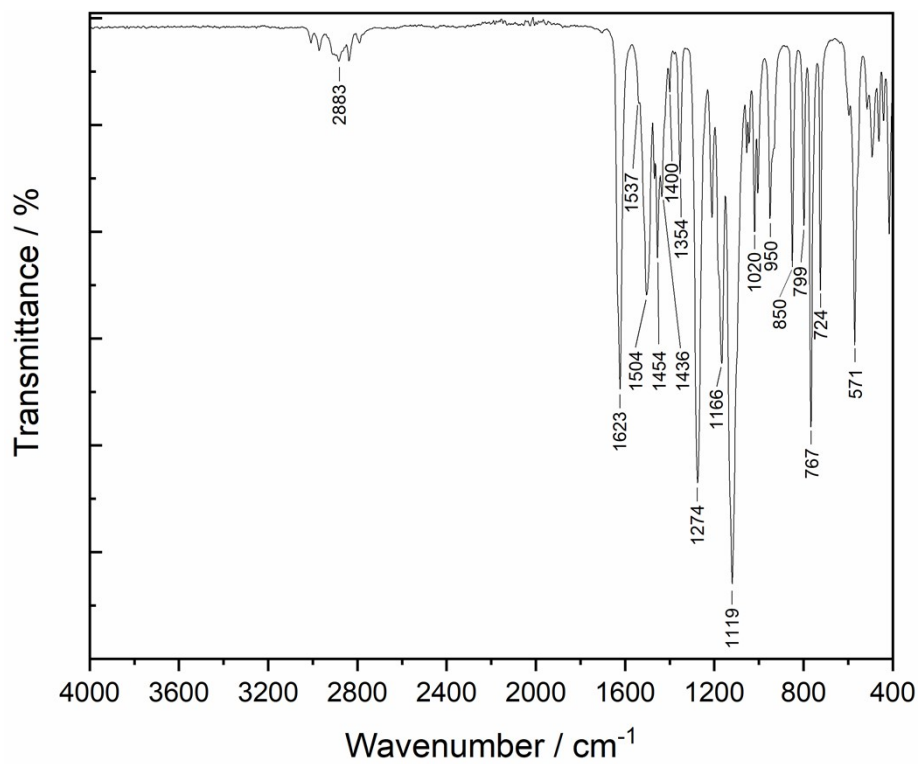


Fig. S6: ATR-IR spectrum of Ni(tfac)₂(TMEDA) **2**.

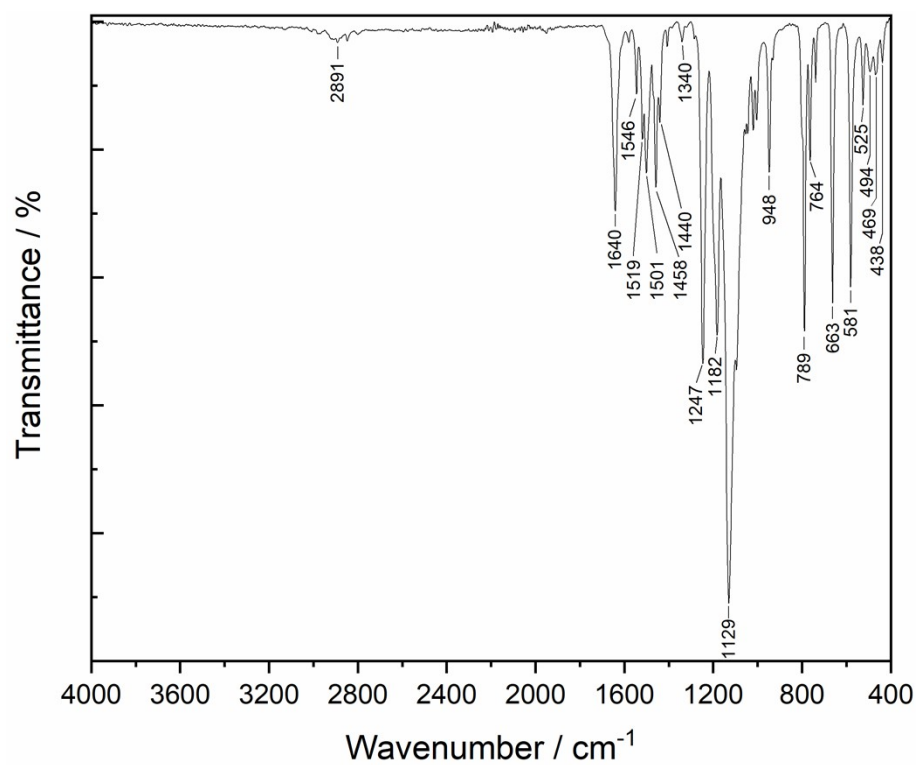


Fig. S7: ATR-IR spectrum of Ni(hfac)₂(TMEDA).

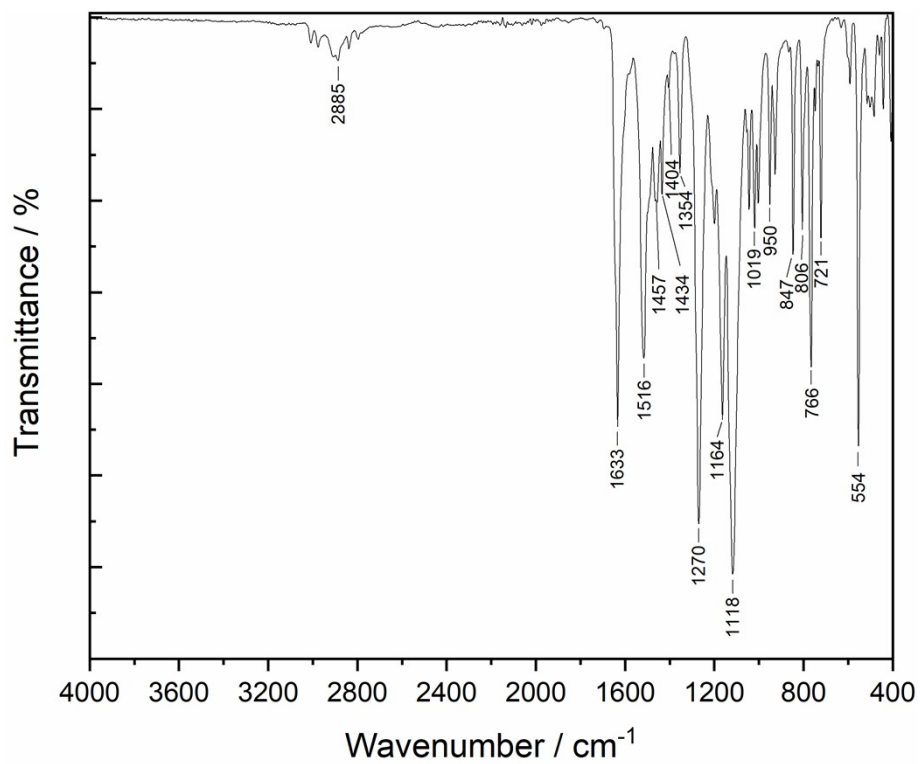


Fig. S8: ATR-IR spectrum of Cu(tfac)₂(TMEDA) **3**.

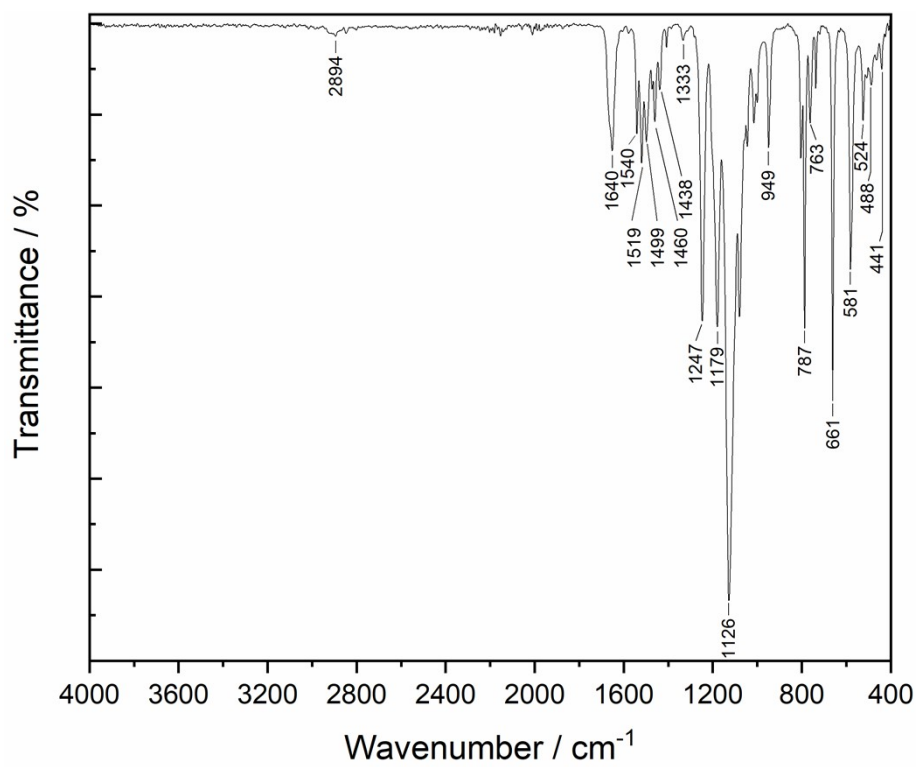


Fig. S9: ATR-IR spectrum of Cu(hfac)₂(TMEDA).

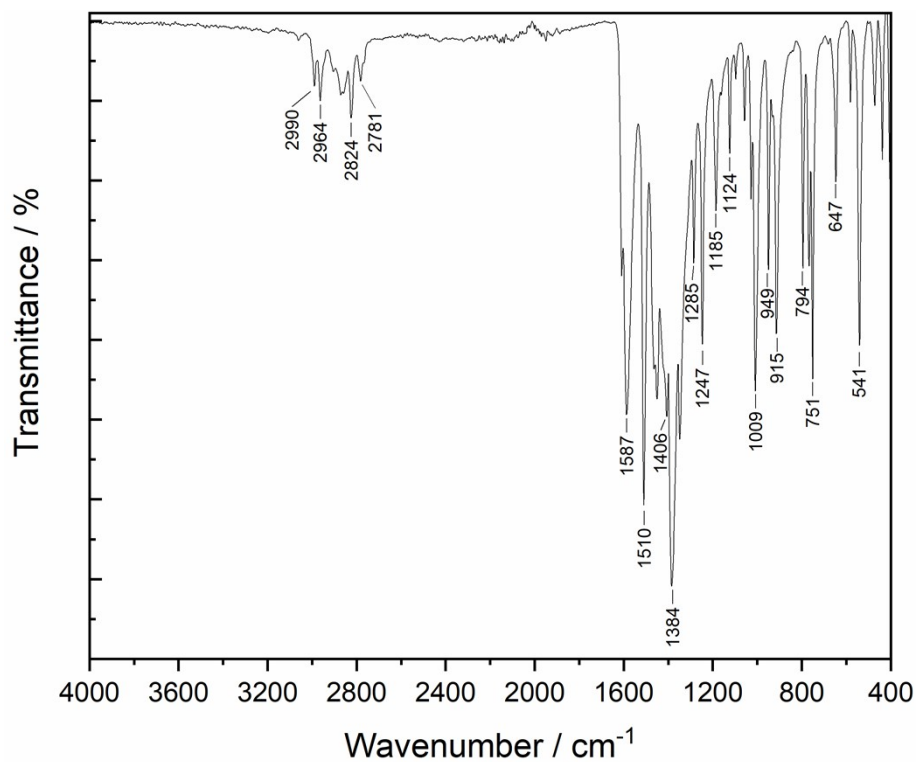


Fig. S10: ATR-IR spectrum of Zn(acac)₂(TMEDA).

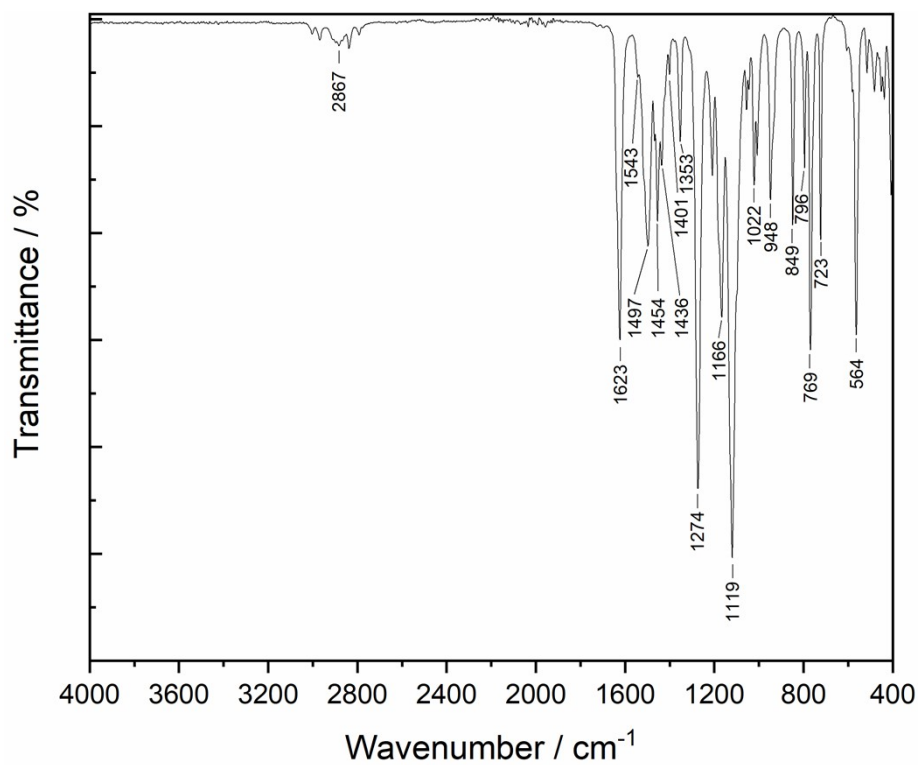


Fig. S11: ATR-IR spectrum of Zn(tfac)₂(TMEDA) 4.

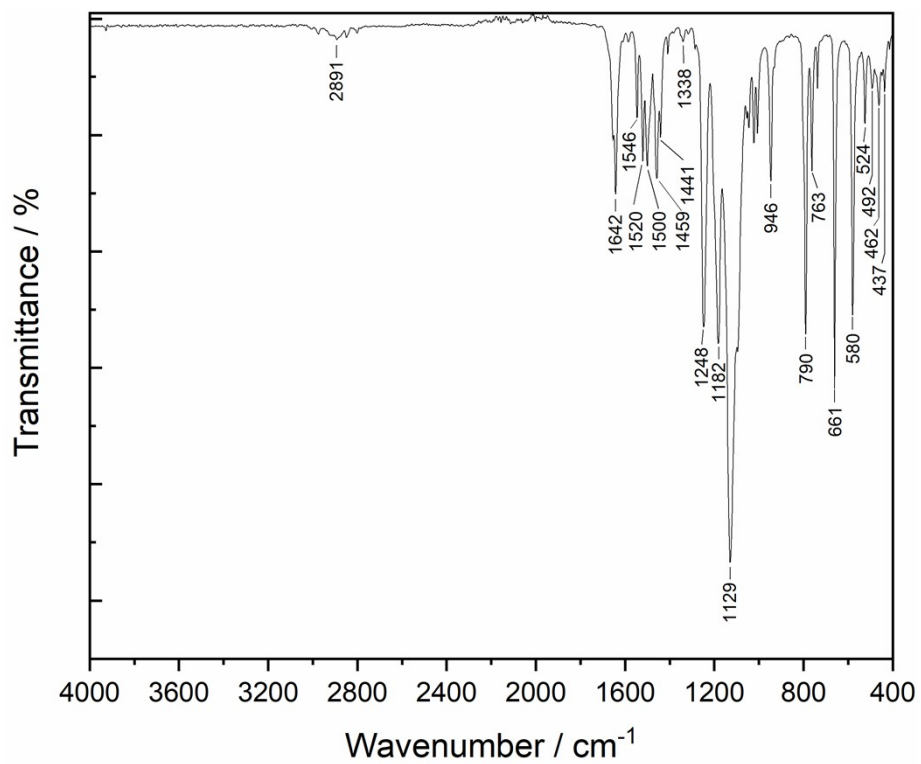


Fig. S12: ATR-IR spectrum of Zn(hfac)₂(TMEDA).

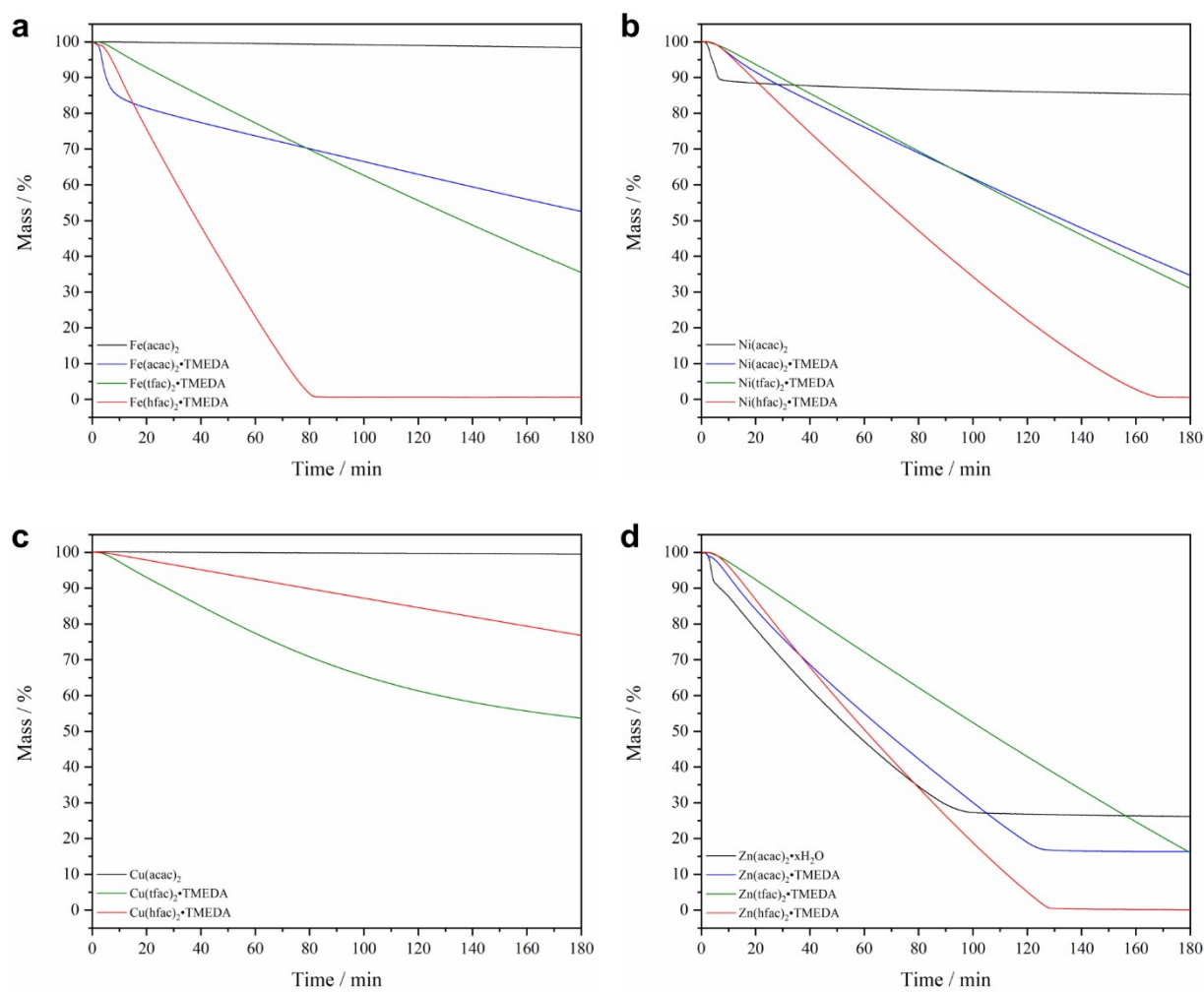


Fig. S13: Isothermal TGA curves (125 °C) for $M(\text{acac})_2$, $M(\text{acac})_2(\text{TMEDA})$, $M(\text{tfac})_2(\text{TMEDA})$ and $M(\text{hfac})_2(\text{TMEDA})$ ($M = \text{Fe}$ (a), Ni (b), Cu (c) and Zn (d)).

For the PXRD analysis of **1-4**, crystalline samples were grinded and measured with Cu-K α radiation. Theoretical X-ray patterns were calculated from the crystal structures using the Mercury software (Version 4.2.0, Cambridge Crystallographic Data Centre) and displayed as vertical red and blue bars. While for **1** a mixture of two polymorphic structures was observed, good agreements were found between the calculated and the experimental X-ray pattern for **2-4**, excluding the presence of polymorphs.

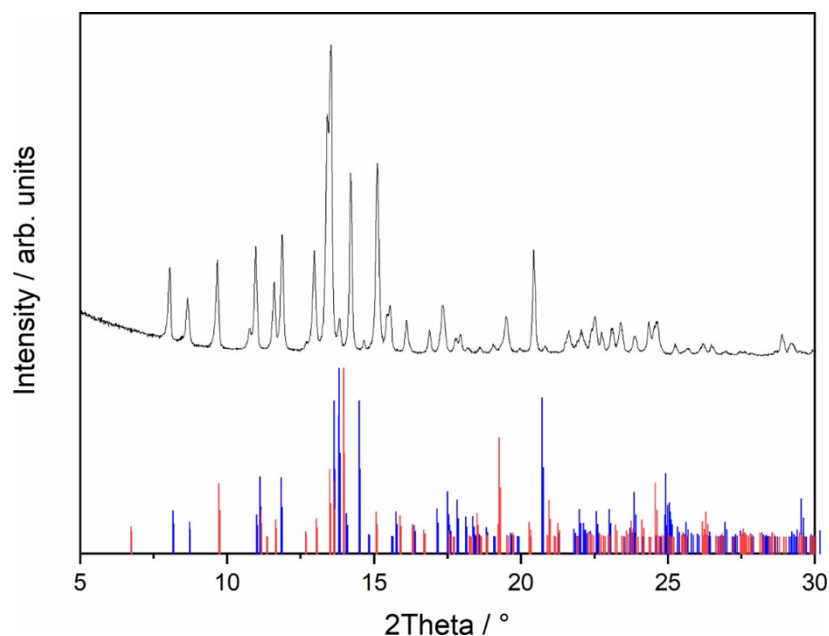


Fig. S14: PXRD of **1**. Calculated position of the reflections from the crystal structure as vertical bars. **1** (red) and Fe(tfac)₂(TMEDA)^[1] (blue).

[1] M. Klotzsche, D. Barreca, L. Bigiani, R. Seraglia, A. Gasparotto, L. Vanin, C. Jandl, A. Pöthig, M. Roverso, S. Bogialli, G. Tabacchi, E. Fois, E. Callone, S. Dirè, C. Maccato, Dalton. Trans.; 2021, 50, 10374–10385.

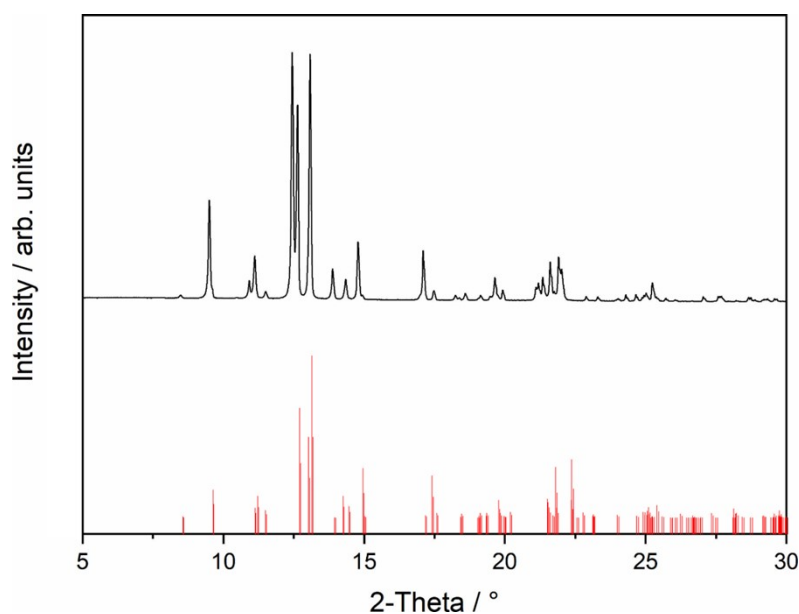


Fig. S15: PXRD of **2**. Calculated position of the reflections from the crystal structure as vertical bars.

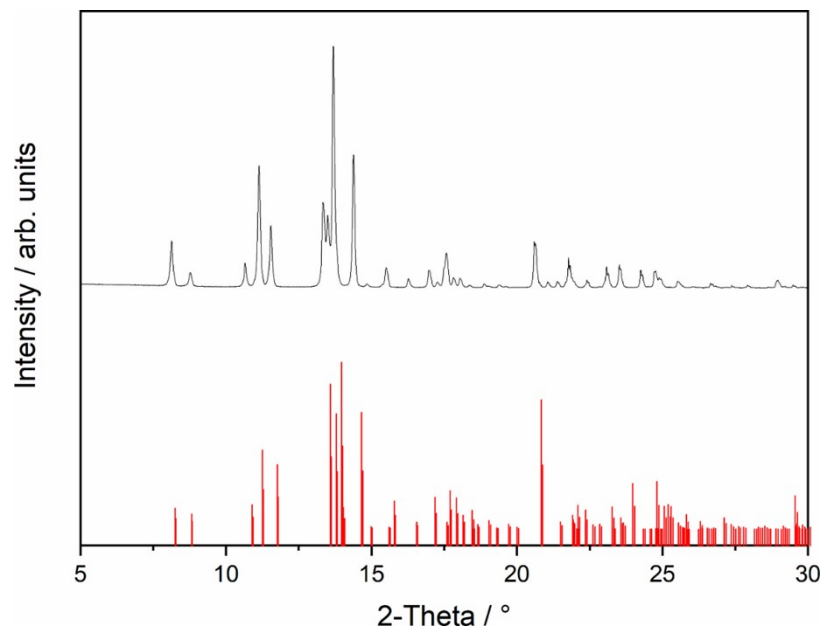


Fig. S16: PXRD of **3**. Calculated position of the reflections from the crystal structure as vertical bars.

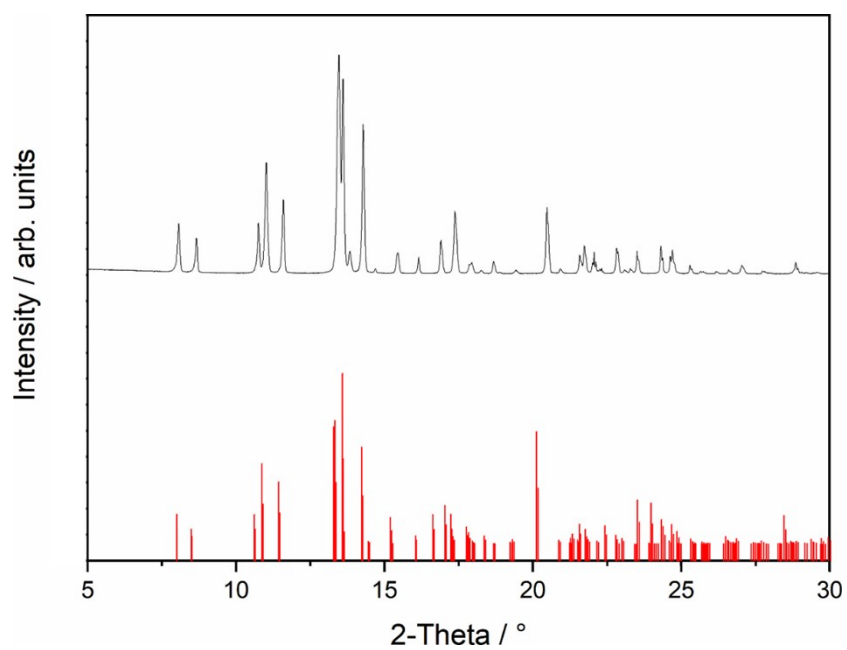


Fig. S17: PXRD of **4**. Calculated position of the reflections from the crystal structure as vertical bars.

Tab. S6: Experimental conditions.

sample name	precursor	evaporation temperature [°C]	deposition temperature [°C]	deposition pressure [mbar]	deposition time [min]	substrate
1_Al	Fe(tfac) ₂ (TMEDA)	100	500	0.35	20	Al ₂ O ₃ (0001)
1_Si	Fe(tfac) ₂ (TMEDA)	100	300-500	0.35	20	Si (100)
2_Al	Ni(tfac) ₂ (TMEDA)	100	500	0.35	20	Al ₂ O ₃ (0001)
2_Si	Ni(tfac) ₂ (TMEDA)	100	300-500	0.35	20	Si (100)
3_Al	Cu(tfac) ₂ (TMEDA)	100	500	0.35	20	Al ₂ O ₃ (0001)
3_Si	Cu(tfac) ₂ (TMEDA)	100	300-500	0.35	20	Si (100)
4_Si	Zn(tfac) ₂ (TMEDA)	100	500	0.35	20	Al ₂ O ₃ (0001)
4_Si	Zn(tfac) ₂ (TMEDA)	100	300-500	0.35	20	Si (100)

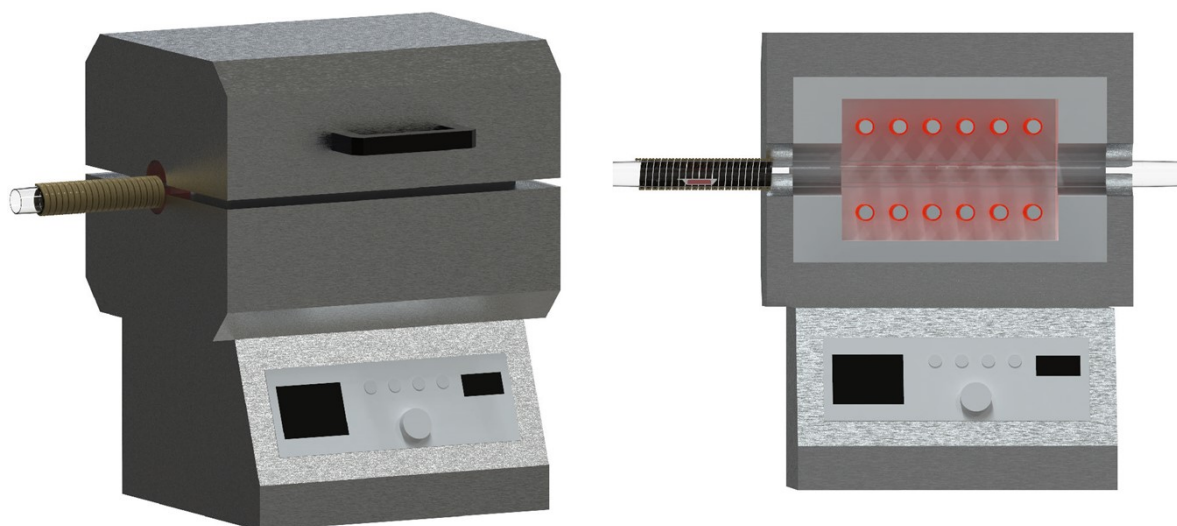


Fig. S18: 3D model of the reactor used in this paper. Side view (left) and front view with cross section (right). Gas supply system and vacuum system are not shown.

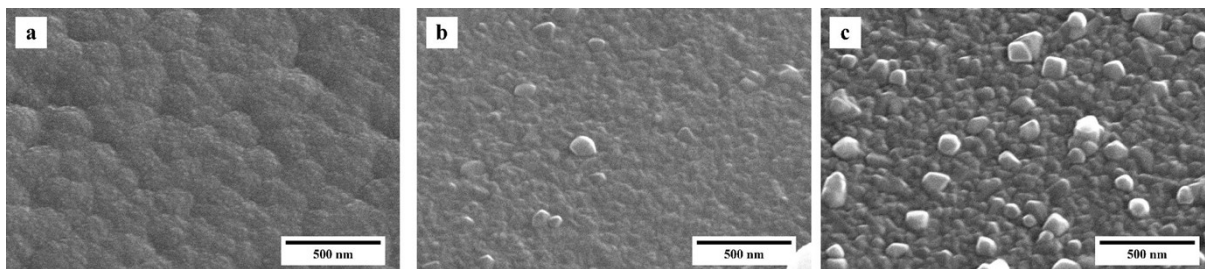


Fig. S19: SEM of **1_Si** at 300 °C (a), 400 °C (b) and 500 °C (c).

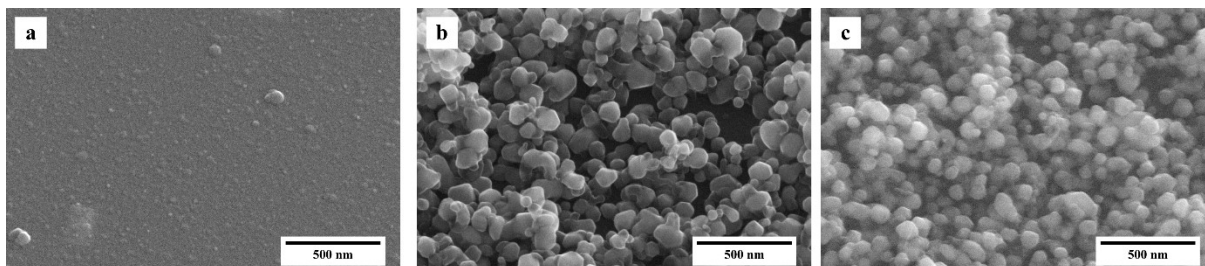


Fig. S20: SEM of **2_Si** at 300 °C (a), 400 °C (b) and 500 °C (c).

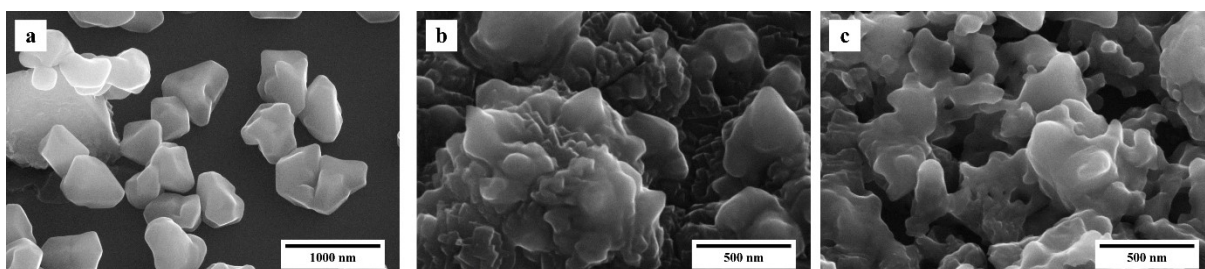


Fig. S21: SEM of **3_Si** at 300 °C (a), 400 °C (b) and 500 °C (c).

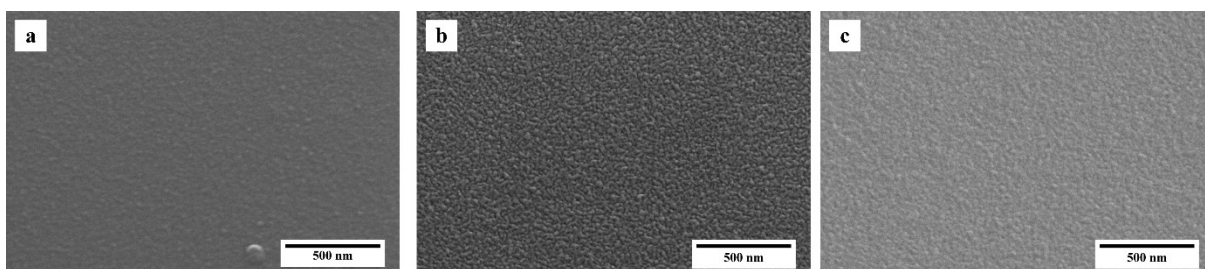


Fig. S22: SEM of **4_Si** at 300 °C (a), 400 °C (b) and 500 °C (c).

Full scale counts: 3944
Integral Counts: 61910

CSR009-Al2O3-B1(1)

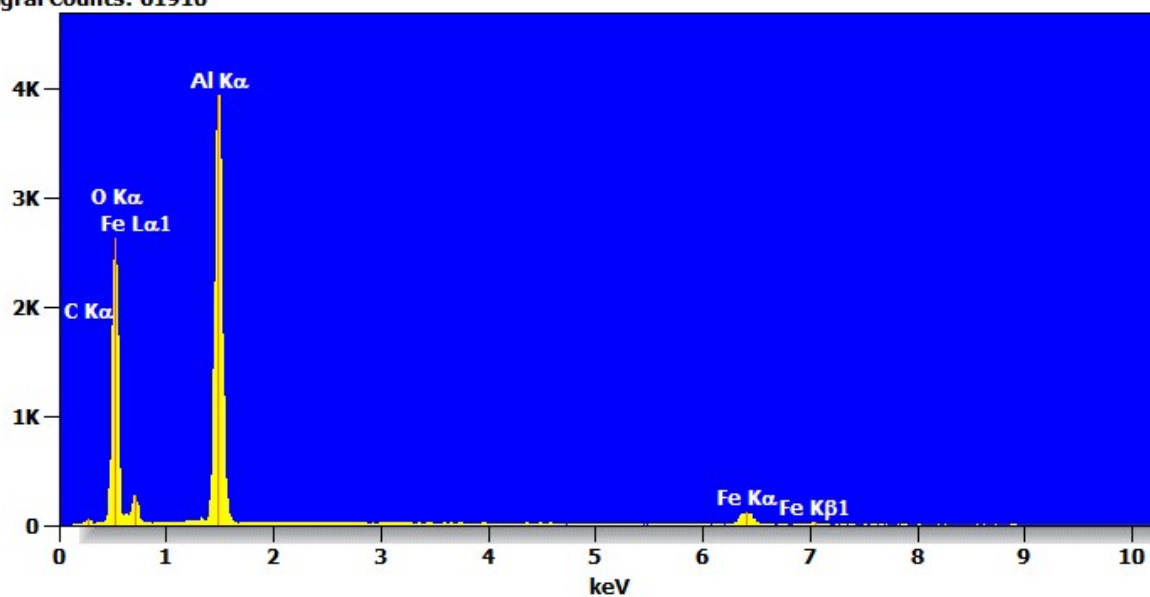


Fig. S23: EDX spectrum of 1_Al.

Full scale counts: 11796
Integral Counts: 177221

CSR010-Al2O3-B1(1)

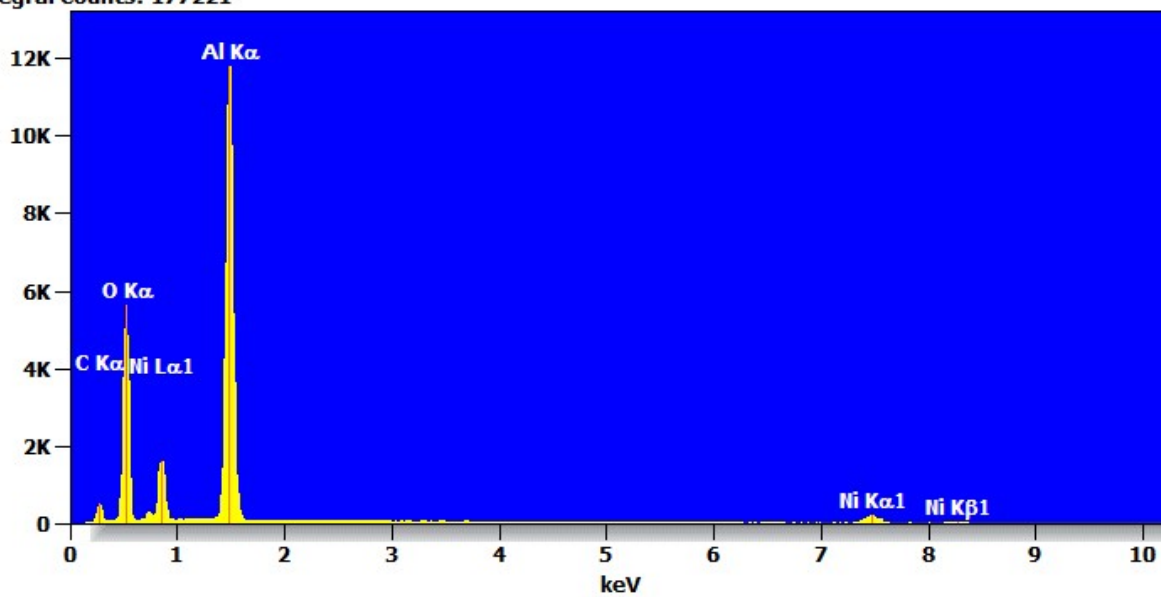


Fig. S24: EDX spectrum of 2_Al.

Full scale counts: 9540
Integral Counts: 167551

CSR011-Al2O3-B1(1)

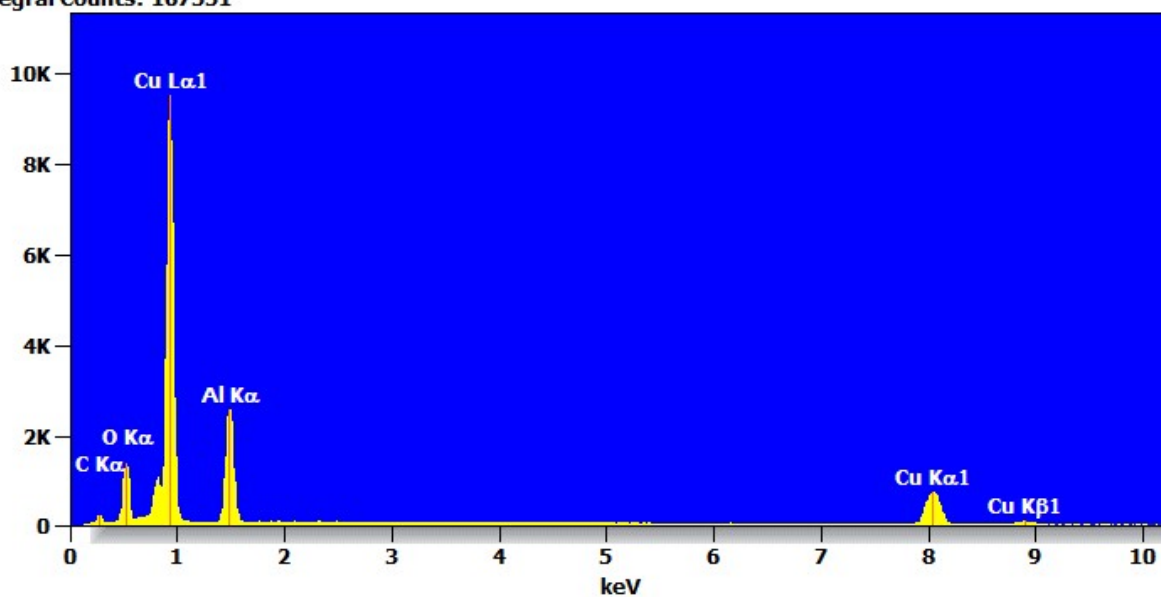


Fig. S25: EDX spectrum of 3_Al.

Full scale counts: 10405
Integral Counts: 175092

CSR012-Al2O3-B1(1)

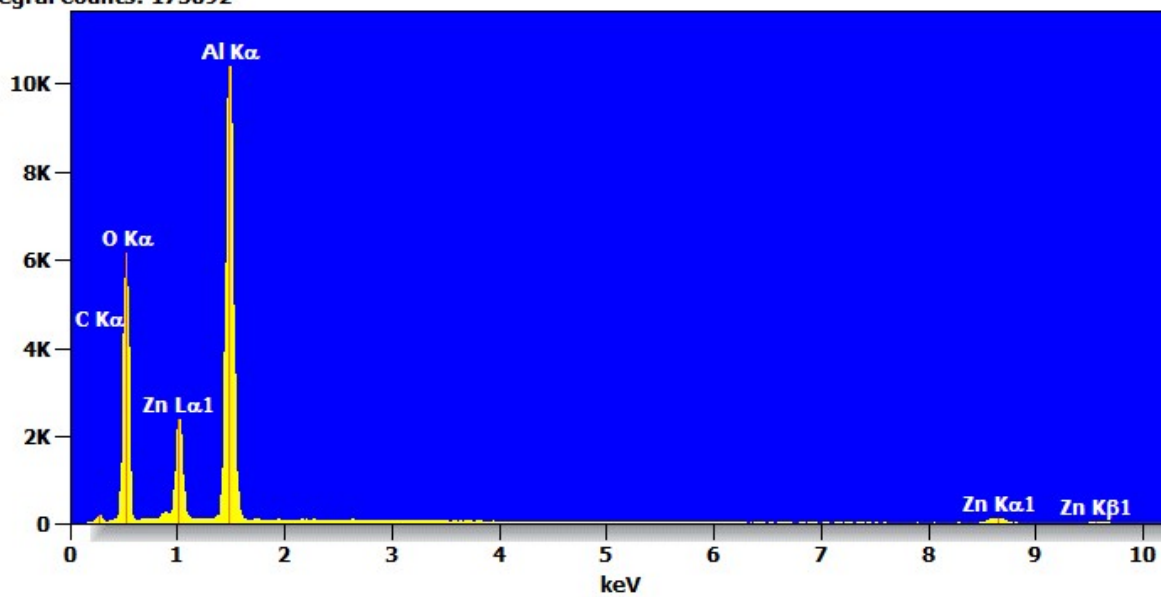


Fig. S26: EDX spectrum of 4_Al.

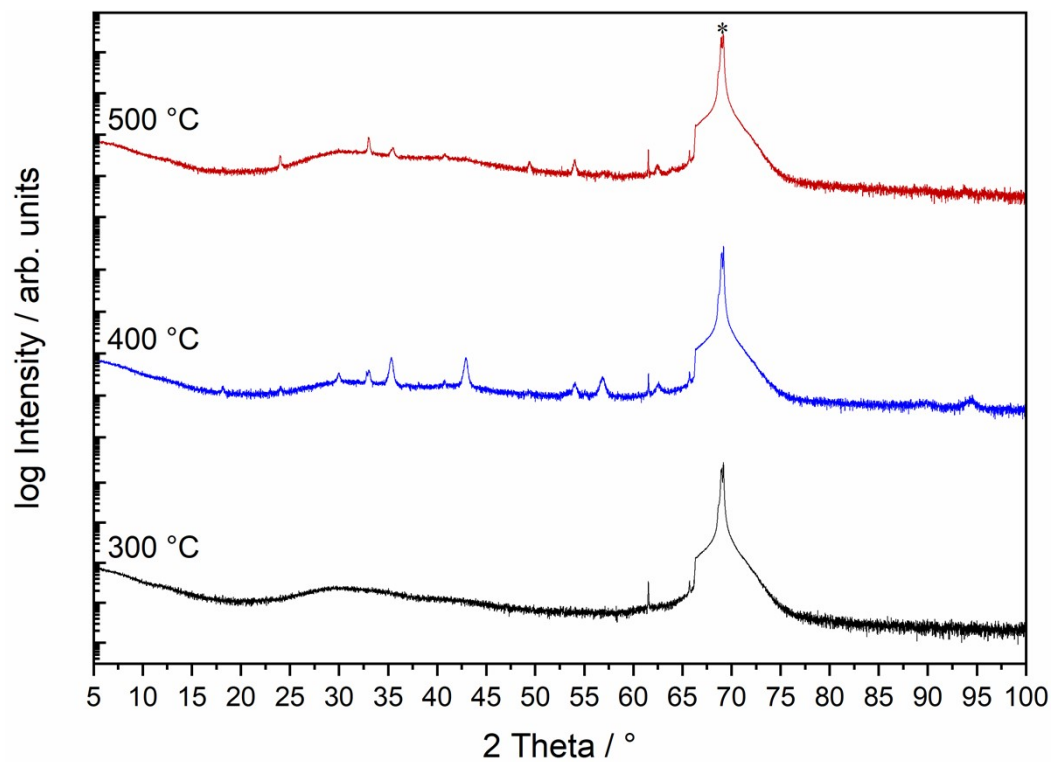


Fig. S27: XRD of 1_Si.

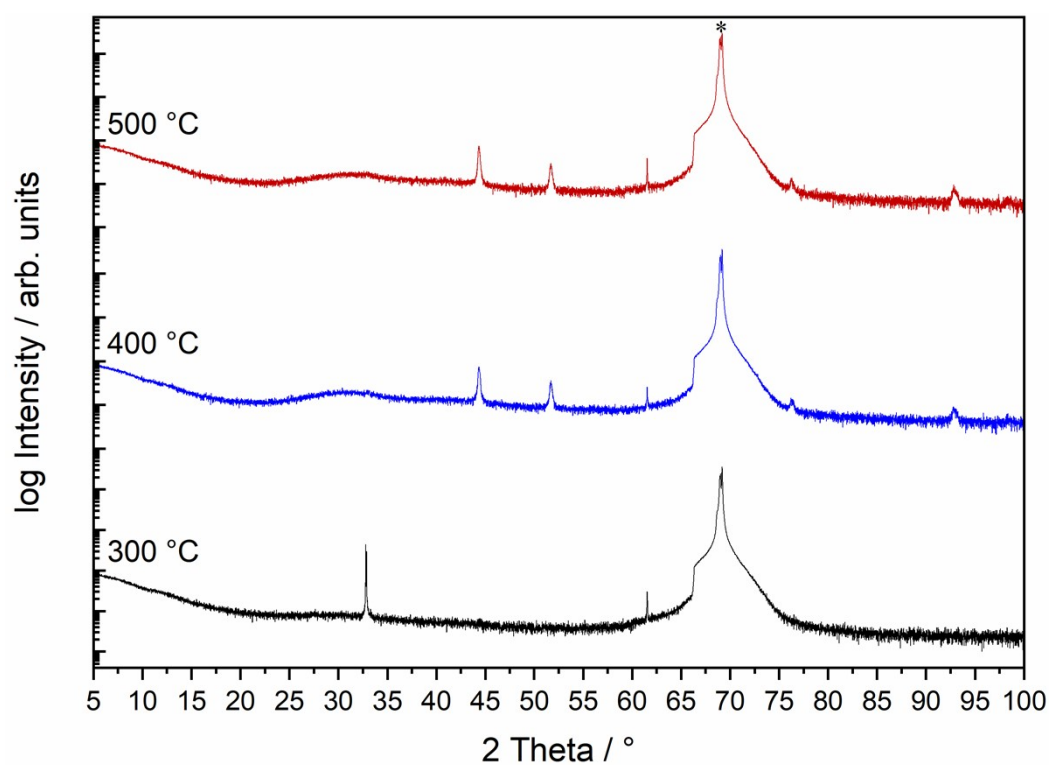


Fig. S28: XRD of 2_Si.

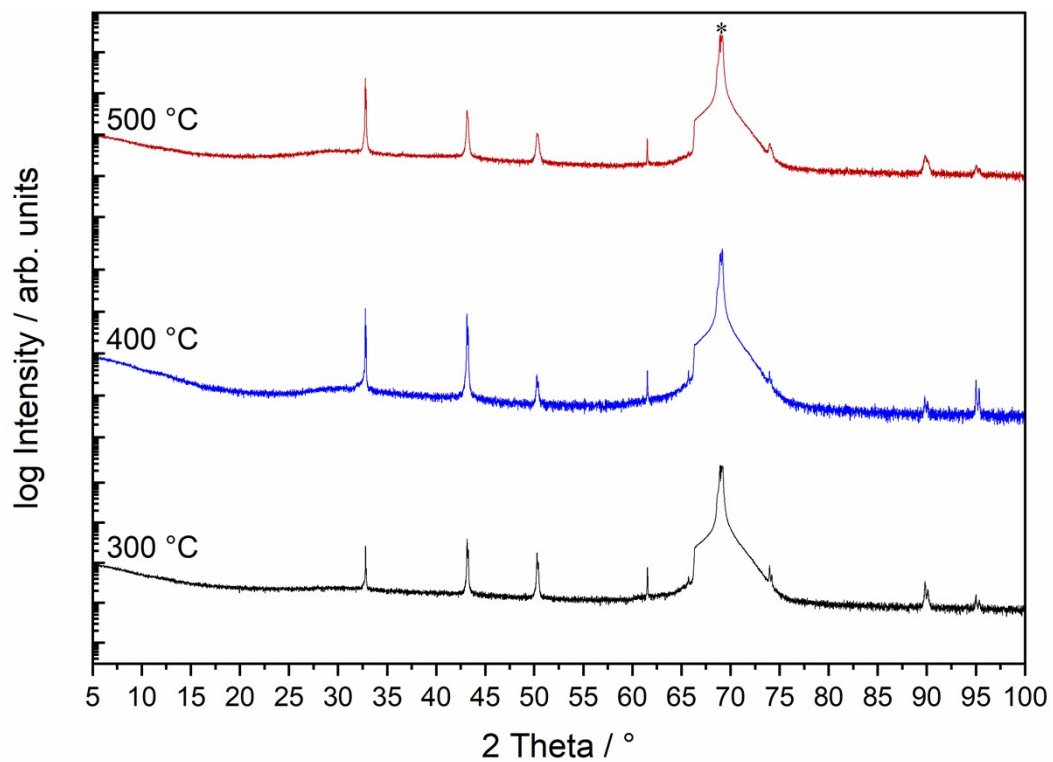


Fig. S29: XRD of 3_Si.

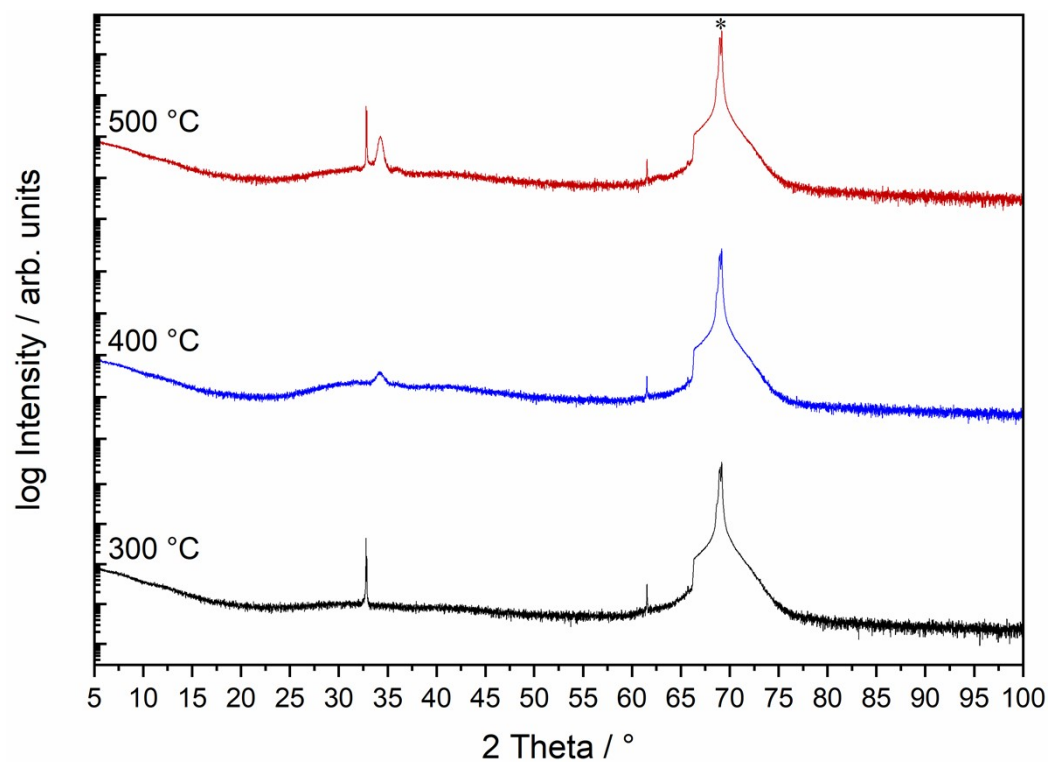


Fig. S30: XRD of 4_Si.

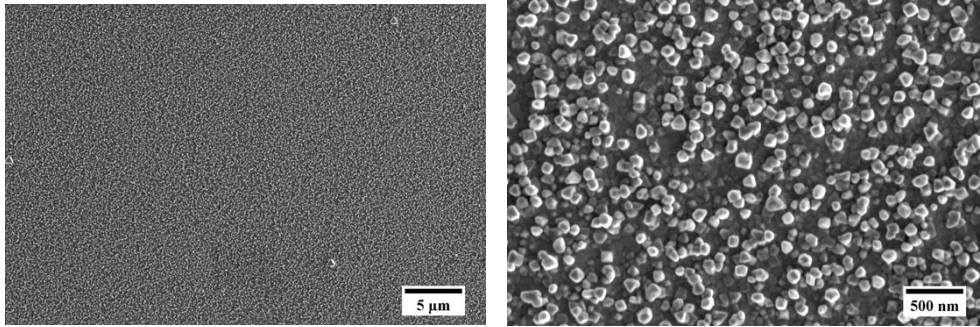


Fig. S31: SEM image of **1_Al**.

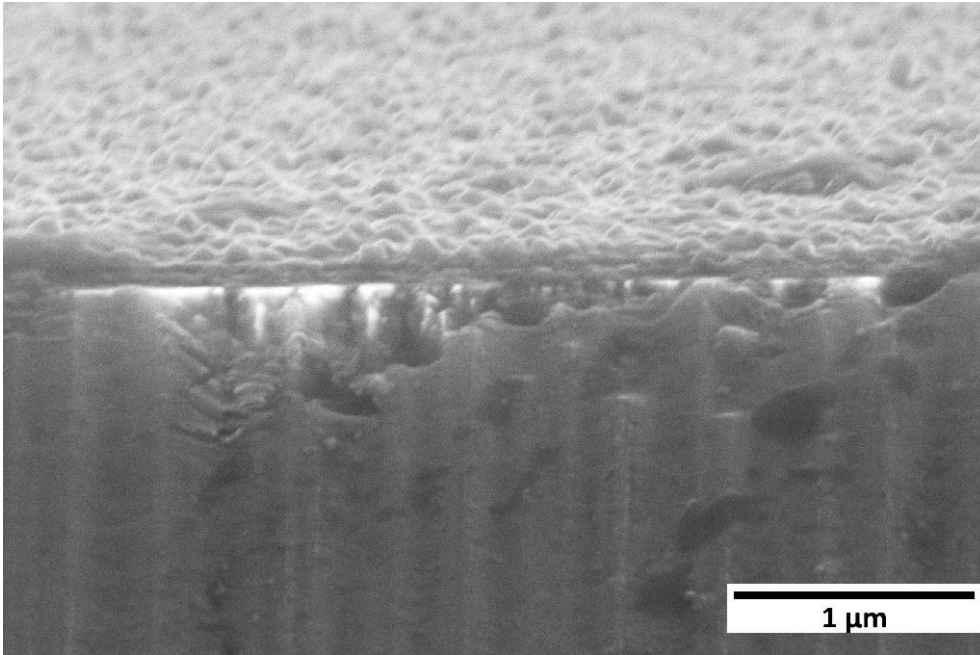


Fig. S32: Cross section SEM image of **1_Al**.

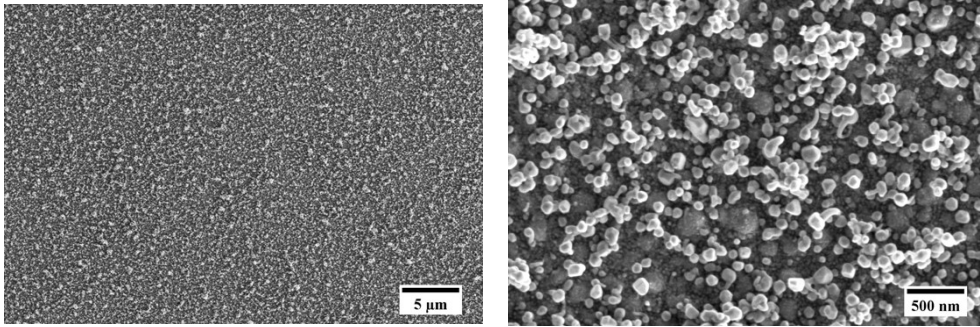


Fig. S33: SEM image of **2_Al**.

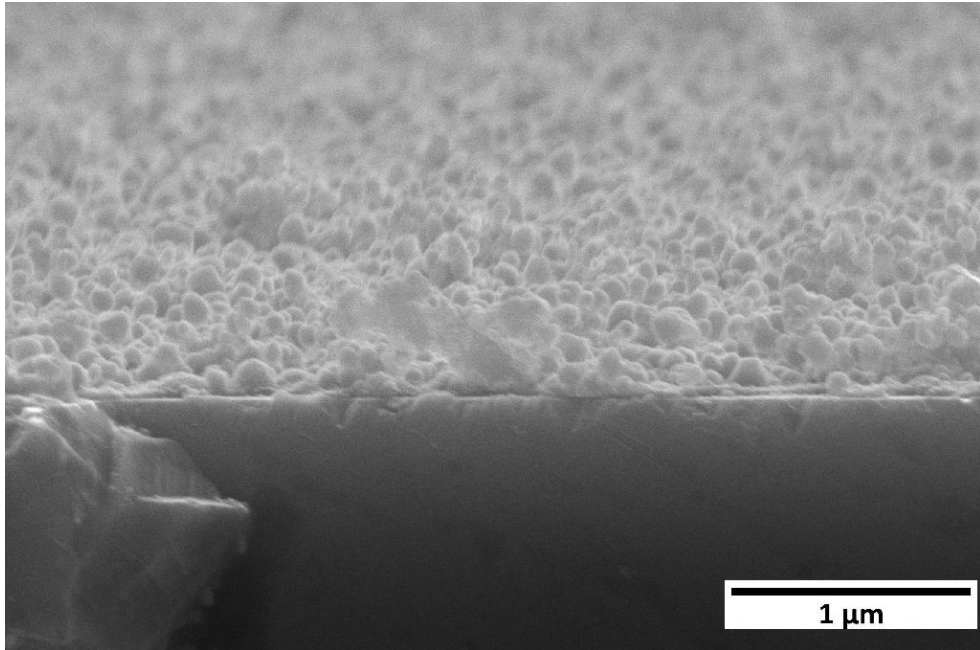


Fig. S34: Cross section SEM image of **2_Al**.

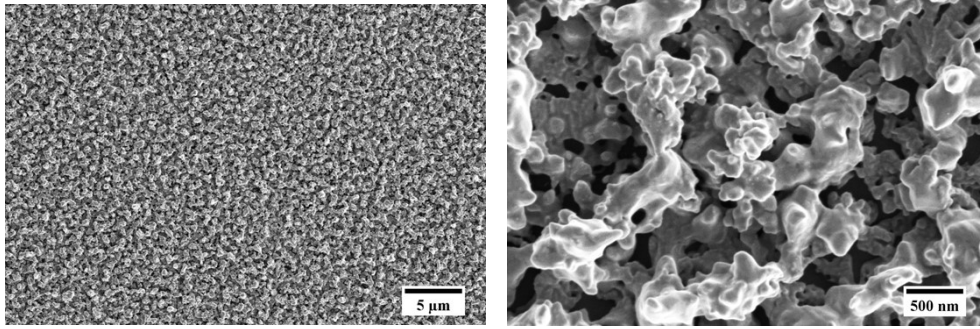


Fig. S35: SEM image of **3_Al**.

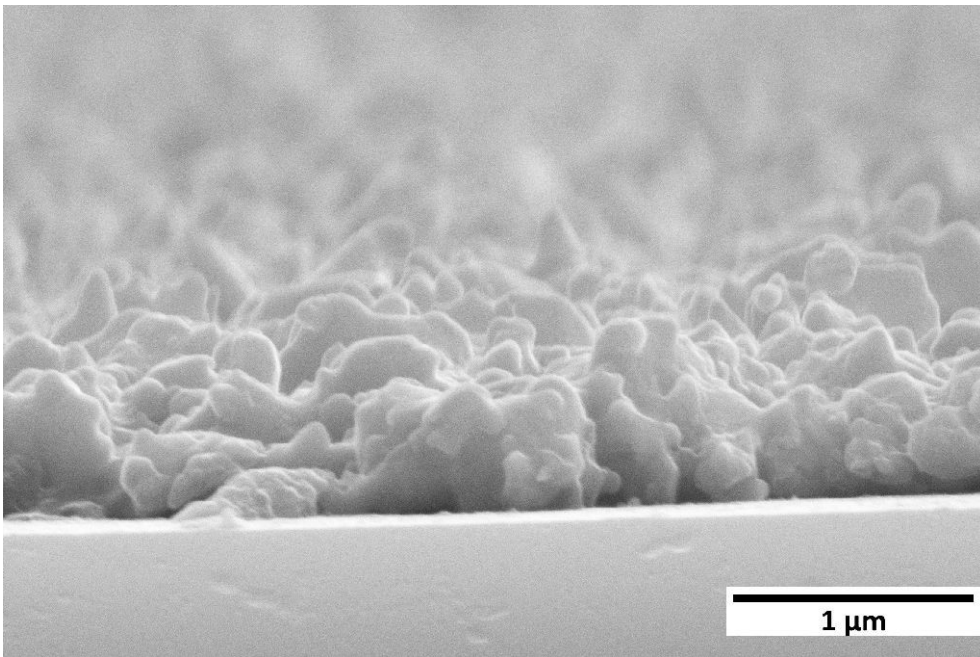


Fig. S36: Cross section SEM image of **3_Al**.

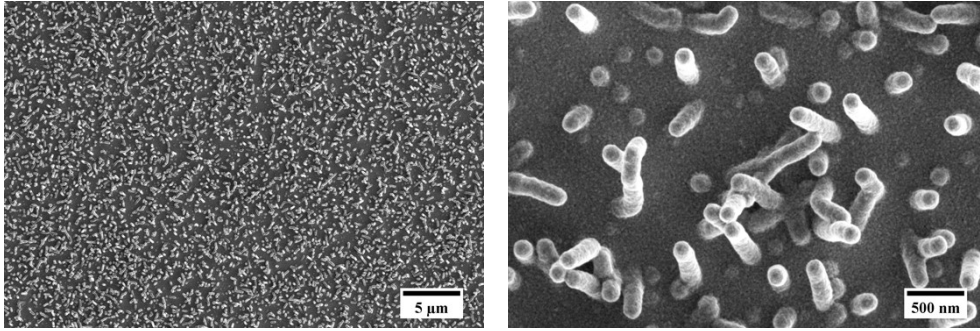


Fig. S37: SEM image of 4_AI.

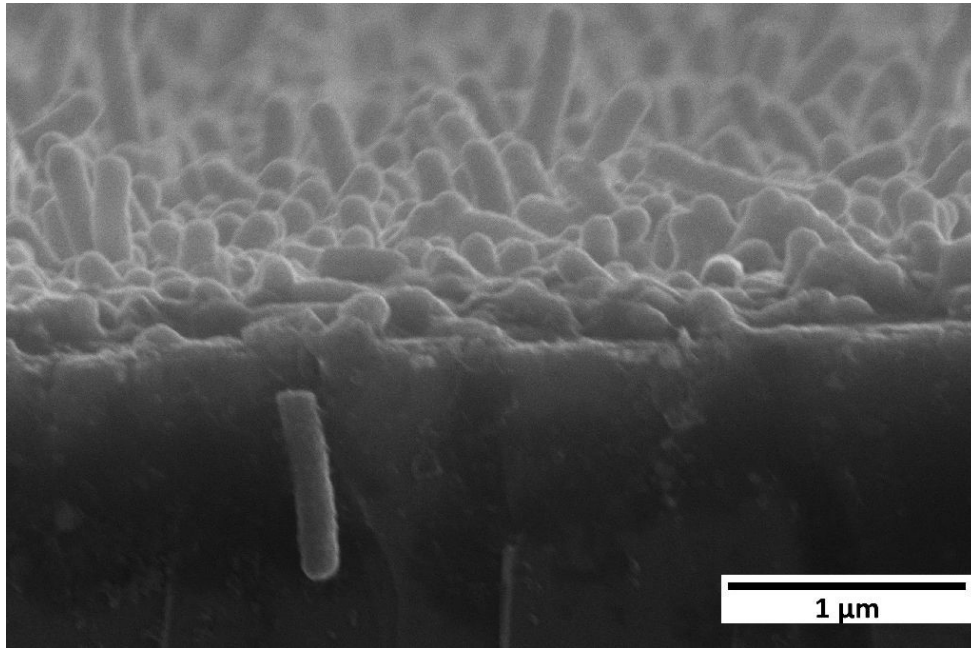


Fig. S38: Cross section SEM image of 4_AI.

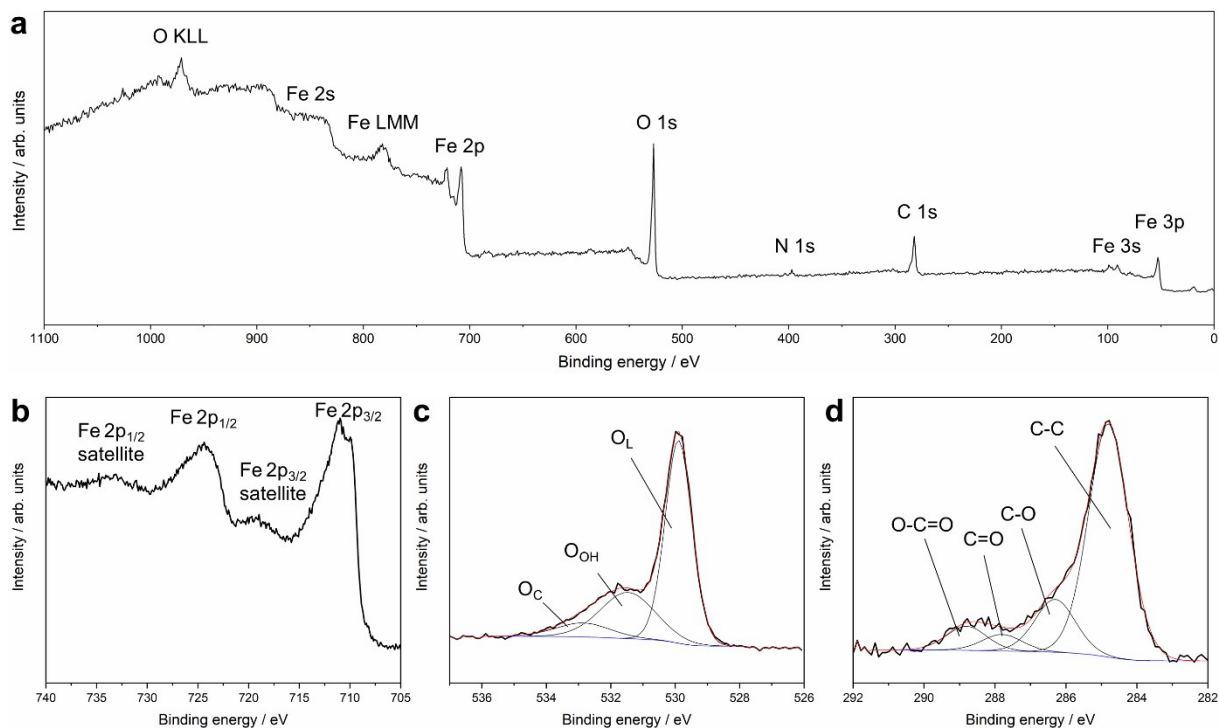


Fig. S39: XPS of 1_AI. Survey (a), Fe 2p (b), O 1s (c) and C 1s (d).

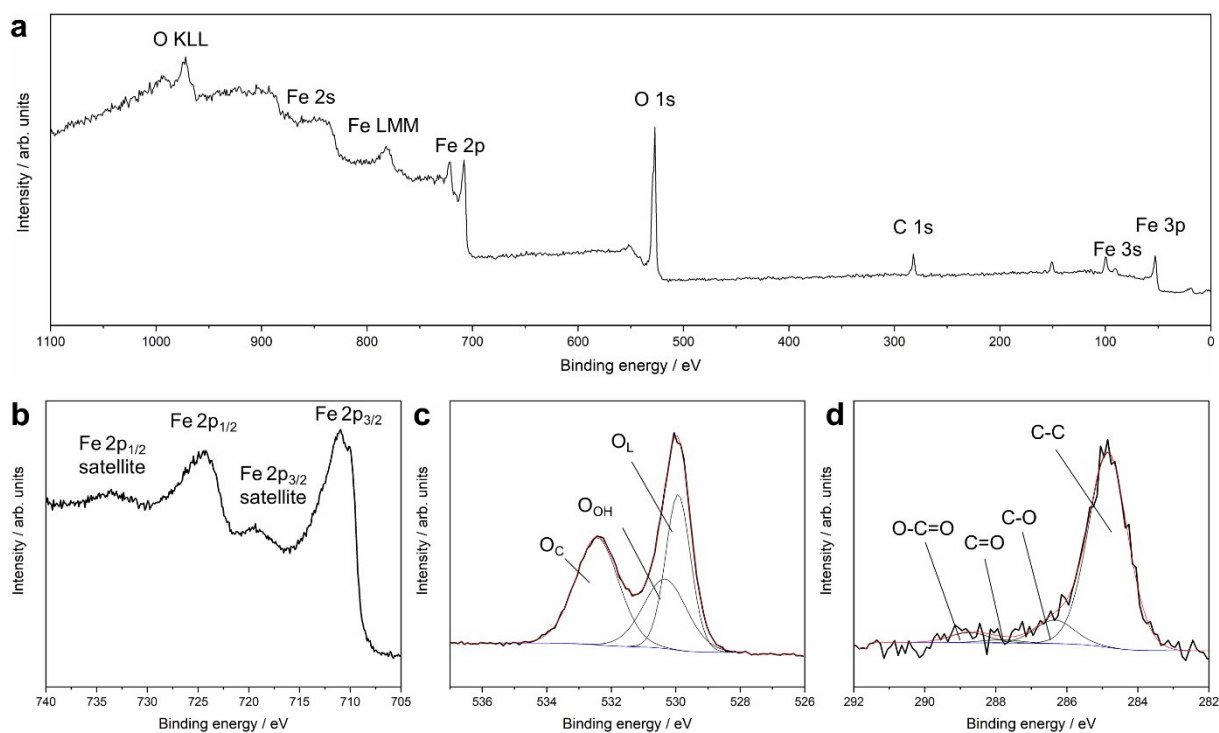


Fig. S40: XPS of 1_AI after calcination. Survey (a), Fe 2p (b), O 1s (c) and C 1s (d).

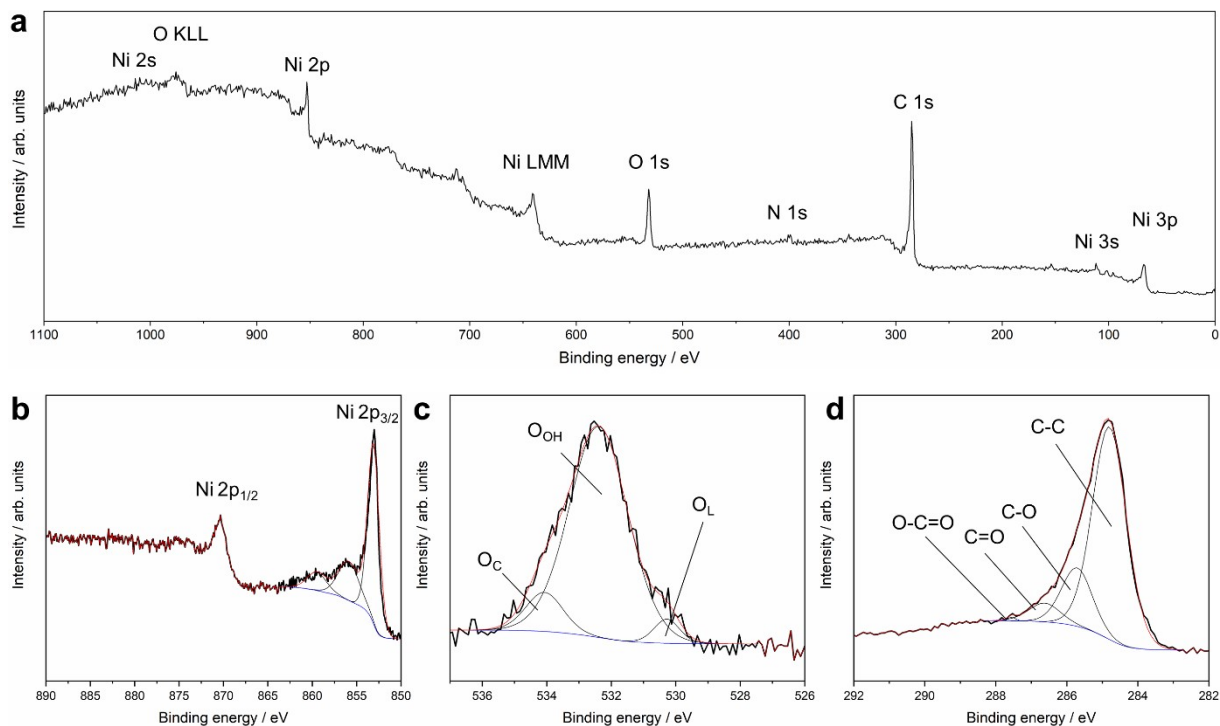


Fig. S41: XPS of **2_AI**. Survey (a), Ni 2p (b), O 1s (c) and C 1s (d).

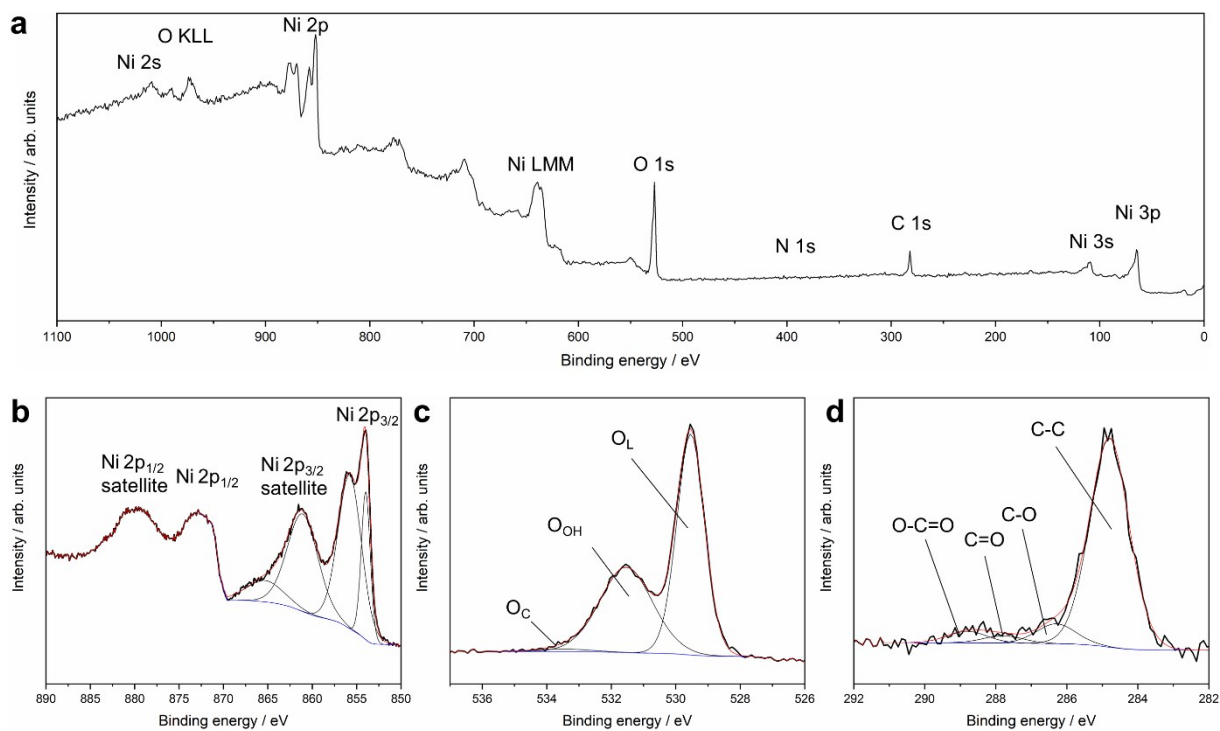


Fig. S42: XPS of **2_AI** after calcination. Survey (a), Ni 2p (b), O 1s (c) and C 1s (d).

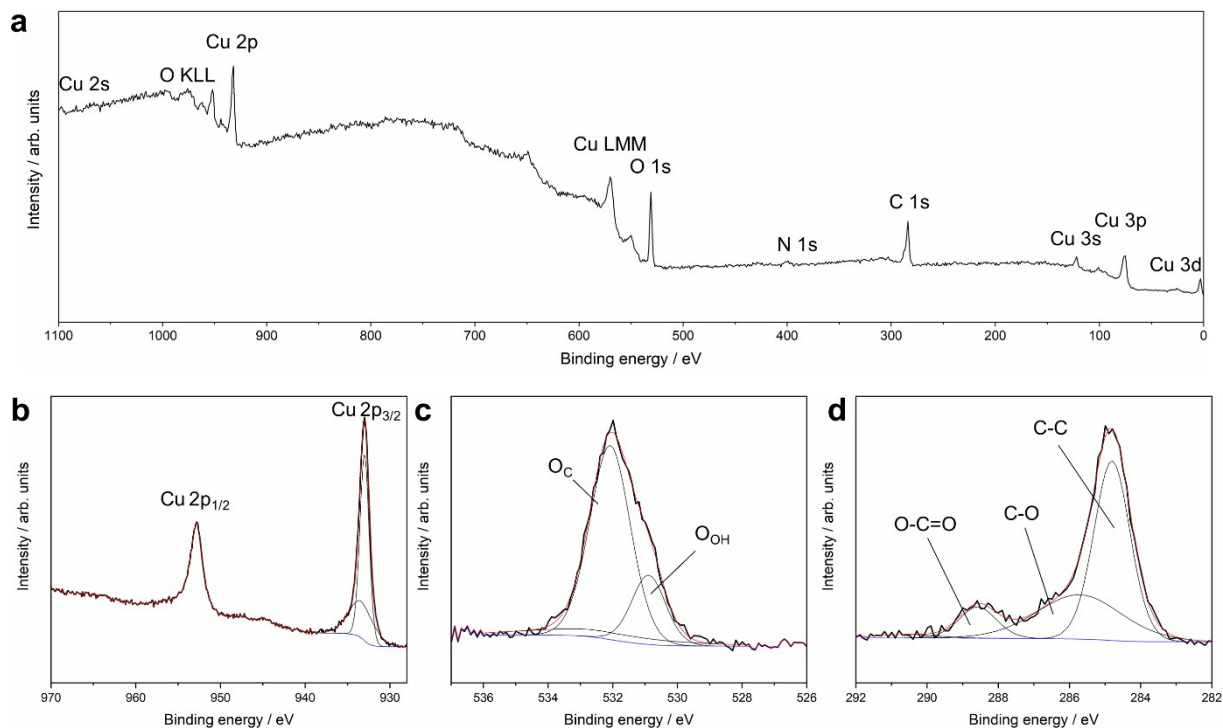


Fig. S43: XPS of **3_AI**. Survey (a), Cu 2p (b), O 1s (c) and C 1s (d).

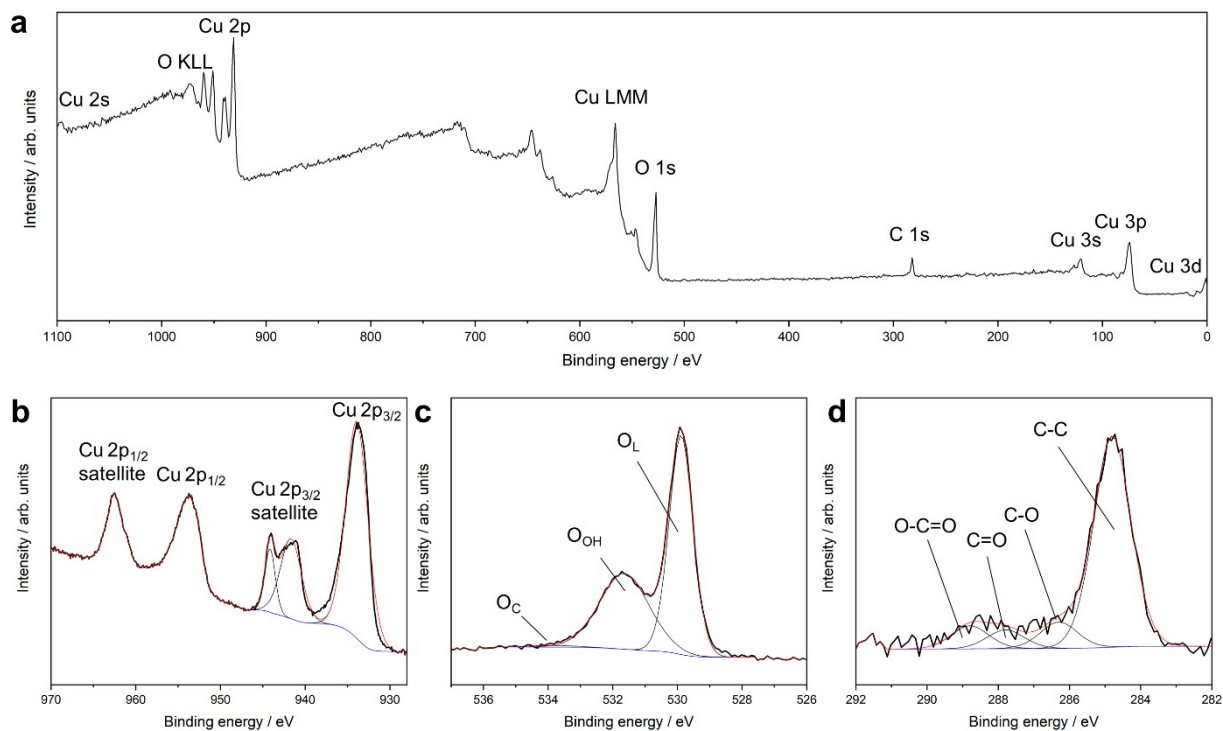


Fig. S44: XPS of **3_AI** after calcination. Survey (a), Cu 2p (b), O 1s (c) and C 1s (d).

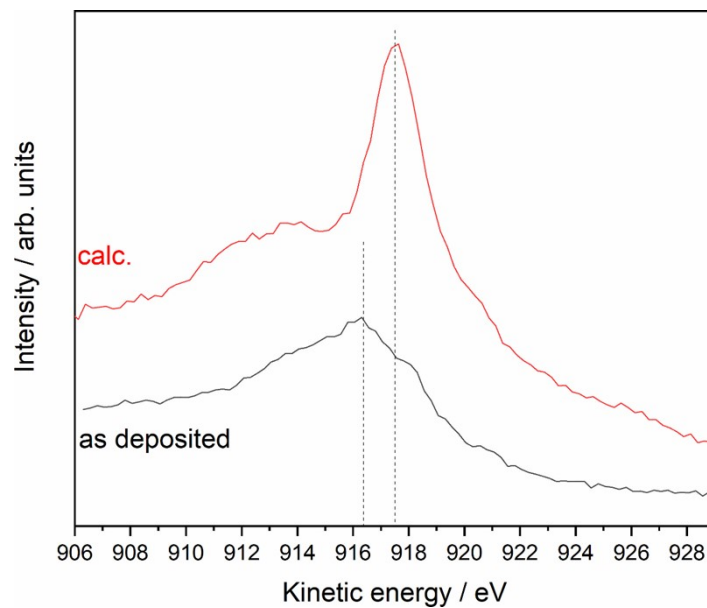


Fig. S45: Cu LMM spectra of **3_AI** before and after calcination.

Tab. S7: Calculation of the mod. Auger parameter for **3_AI**

	Cu 2p _{3/2} (eV)	Zn LMM (eV)	Mod. Auger parameter (eV)	Mod. Auger parameter (eV) Reference ^[2]
3_AI	933.0	916.4	1849.4	1849.2 (Cu ₂ O)
3_AI_calc	933.7	917.6	1851.3	1851.3 (CuO)

[2] M. C. Biesinger, Surf. Interface Anal., 2017, 49, 1325–1334.

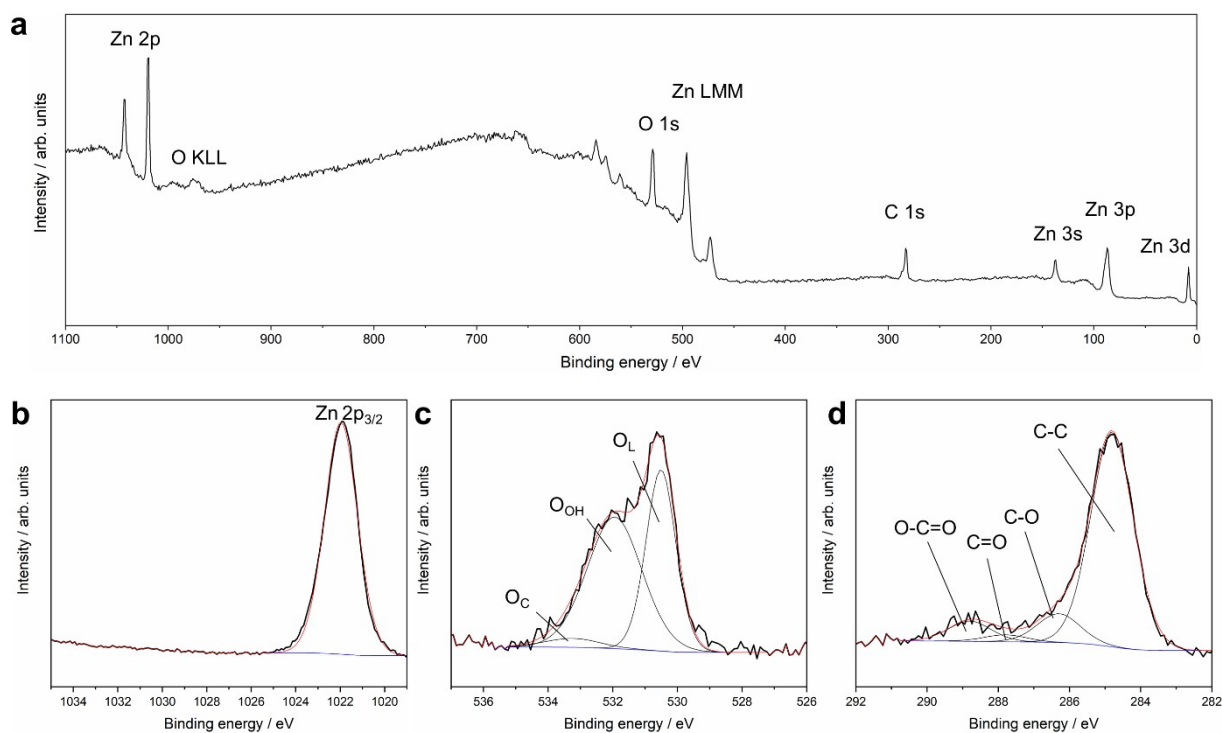


Fig. S46: XPS of **4_AI**. Survey (a), Zn 2p (b), O 1s (c) and C 1s (d).

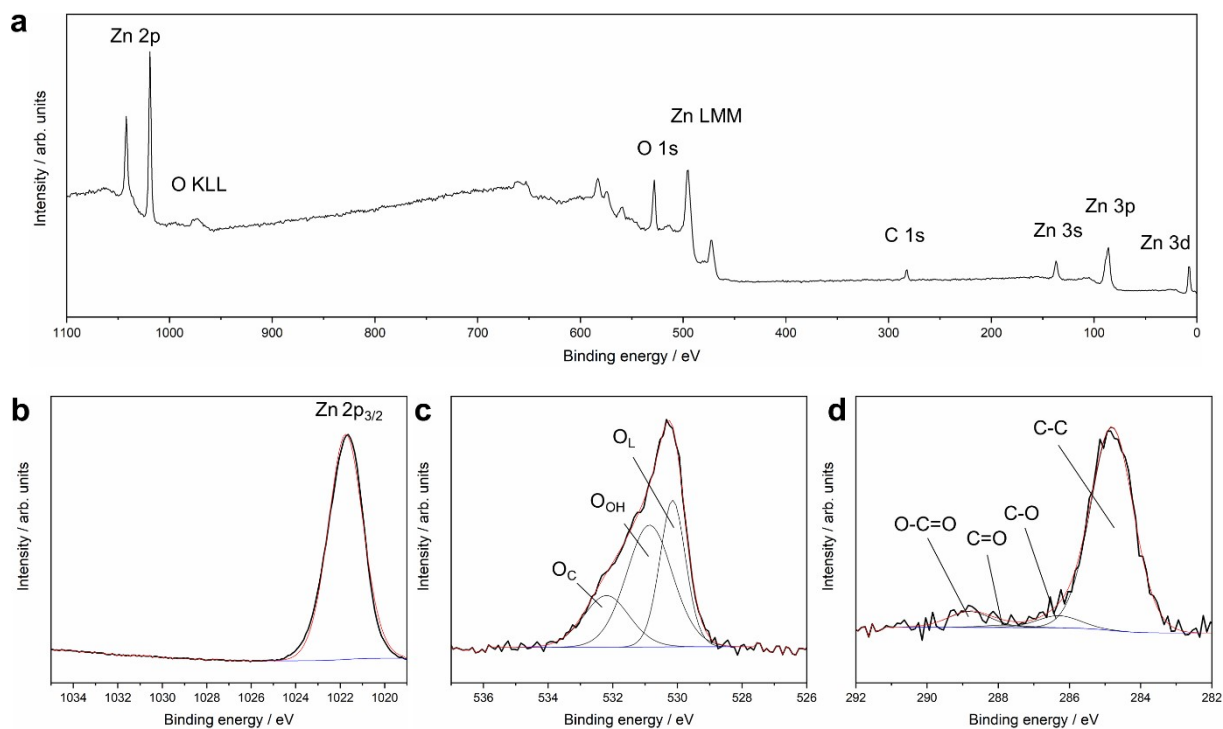


Fig. S47: XPS of **4_AI** after calcination. Survey (a), Zn 2p (b), O 1s (c) and C 1s (d).

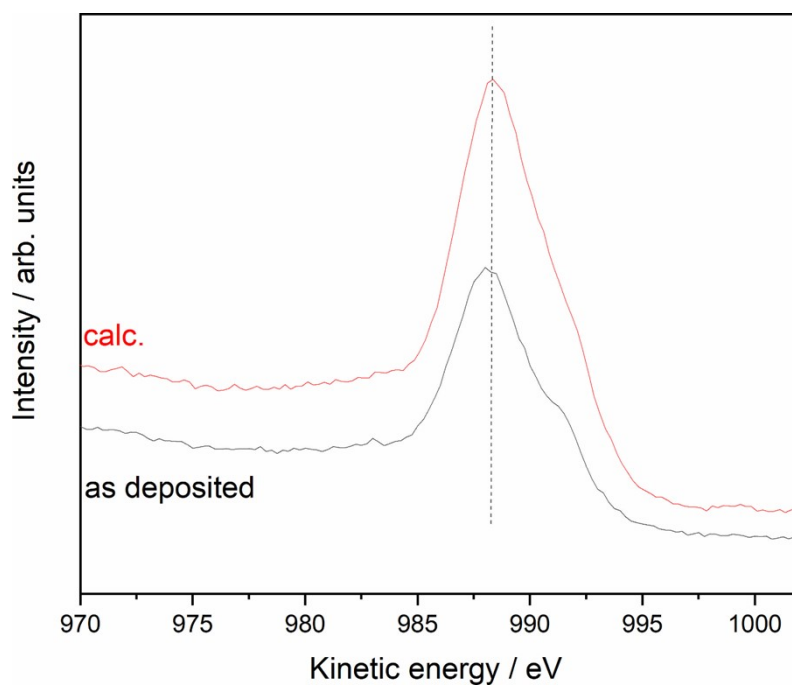


Fig. S48: Zn LMM spectra of **4_AI** before and after calcination.

Tab. S8: Calculation of the mod. Auger parameter for **3_AI**

	Zn 2p _{3/2} (eV)	Zn LMM (eV)	Mod. Auger parameter (eV)	Mod. Auger parameter (eV) Reference ^[3]
4_AI	1021.9	988.0	2009.9	2010.4 (ZnO)
4_AI_calc	1021.7	988.3	2010.0	2010.4 (ZnO)

[3] M. C. Biesinger, L. W. M. Lau, A. R. Gerson, R. S. C. Smart, *Appl. Surf. Sci.* **2010**, 257, 887–898.